Flood Vulnerability Assessment Using the Triangular Fuzzy Number-based Analytic Hierarchy Process and Support Vector Machine Model for the Belt and Road Region

Yu Duan
School of Civil Engineering and Geomatics, Southwest Petroleum University, Chengdu, 640500, China
https://orcid.org/0000-0002-3620-3251

Junnan Xiong (✉ xiongjn@swpu.edu.cn)
School of Civil Engineering and Geomatics, Southwest Petroleum University, Chengdu, 640500, China; State Key Laboratory of Resources and Environmental Information System, Institute of Geographic Sciences and Natural Resources Research, CAS, Beijing, 100101, China

Weiming Cheng
State Key Laboratory of Resources and Environmental Information System, Institute of Geographic Sciences and Natural Resources Research, CAS, Beijing, 100101, China; University of Chinese Academy of Sciences, Beijing, 100049, China

Nan Wang
State Key Laboratory of Resources and Environmental Information System, Institute of Geographic Sciences and Natural Resources Research, CAS, Beijing, 100101, China; University of Chinese Academy of Sciences, Beijing, 100049, China

Yi Li
Aerospace Information Research Institute, CAS, Beijing, 100094, China

Yufeng He
School of Civil Engineering and Geomatics, Southwest Petroleum University, Chengdu, 640500, China

Jun Liu
School of Civil Engineering and Geomatics, Southwest Petroleum University, Chengdu, 640500, China

Wen He
School of Civil Engineering and Geomatics, Southwest Petroleum University, Chengdu, 640500, China

Gang Yang
School of Civil Engineering and Geomatics, Southwest Petroleum University, Chengdu, 640500, China

---

Research Article

Keywords: flood, vulnerability, triangular fuzzy number-based analytic hierarchy process, support vector machine, the Belt and Road region

Posted Date: March 24th, 2021

DOI: https://doi.org/10.21203/rs.3.rs-340694/v1

Version of Record: A version of this preprint was published at Natural Hazards on July 25th, 2021. See the published version at https://doi.org/10.1007/s11069-021-04946-9.

Flood Vulnerability Assessment using the Triangular Fuzzy Number-Based Analytic Hierarchy Process and Support Vector Machine Model for the Belt and Road Region

Yu Duan[1], Junnan Xiong[1,2]*, Weiming Cheng[2,3], Nan Wang[2,3], Yi Li[4], Yufeng He[1], Jun Liu[1], Wen He[1], Gang Yang[1]

1 School of Civil Engineering and Geomatics, Southwest Petroleum University, Chengdu, 640500, China;

2 State Key Laboratory of Resources and Environmental Information System, Institute of Geographic Sciences and Natural Resources Research, CAS, Beijing,100101, China;

3 University of Chinese Academy of Sciences, Beijing 100049, China;

4 Aerospace Information Research Institute, CAS, Beijing 100094, China;

Junnan Xiong*: E-mail: xiongjn@swpu.edu.cn

Yu Duan: E-mail: 201922000658@stu.swpu.edu.cn

Weiming Cheng: E-mail: chengwm@lreis.ac.cn

Nan Wang: E-mail: wangnd.17b@igsnrr.ac.cn

Yi Li: E-mail: liyi@aircas.ac.cn

Yufeng He: E-mail: 201922000656@stu.swpu.edu.cn

Jun Liu: E-mail: 201922000655@stu.swpu.edu.cn

Wen He: E-mail: 201922000663@stu.swpu.edu.cn

Gang Yang: E-mail: 201922000664@stu.swpu.edu.cn

***Corresponding author:**

Junnan Xiong

Tel.: 86-135-4122-3403

E-mail.: xiongjn@swpu.edu.cn

Abstract: Floods are one of the most serious natural disasters. Flood disaster losses in the developing countries in the Belt and Road region are more than twice the global average. However, to date, the extent of the vulnerability of the Belt and Road Region remains poorly understood. This study sought to address this knowledge gap. In this study, the flood vulnerability throughout the Belt and Road region was evaluated by adopting the triangular fuzzy number-based analytic hierarchy process (TFN-AHP) and the support vector machine (SVM) model. According to the results, the vulnerability of most areas (47,105,300 km^2) is low or extremely low, accounting for 93% of the Belt and Road region. The highly-vulnerable areas (accounting for 3.54%) are primarily concentrated in the southern and eastern parts of China, northern India, most areas of Bangladesh, the Indus Valley in Pakistan, the Nile River Basin in Egypt, and the central region of Indonesia. From a local perspective, in the Belt and Road region, many major cities have higher vulnerability, such as Beijing, Shanghai, and Hong Kong. Compared with the three typical cities, the level of vulnerability in other cities (including Bangkok, Bangalore, Cairo, Riyadh, and Moscow) is lower, due to their higher disaster reduction capability. Thus, these highly vulnerable regions and cities coincide with areas characterized by frequent economic activity and dense populations. Based on these results, this study provides scientific and technological evidence for the prevention and mitigation of flood disasters in the countries along the Belt and Road region.

Keywords: flood; vulnerability; triangular fuzzy number-based analytic hierarchy process; support vector machine; the Belt and Road region

Declarations

We confirm that this manuscript has not been published elsewhere and is not under consideration by another journal. All authors have approved the manuscript, including authorship and order of authorship, and agree with submission to ***Nature Hazards***.

Funding. This study is supported by Strategic Priority Research Program of the Chinese Academy of Sciences (Grant No. XDA20030302), Key R & D project of Sichuan Science and Technology Department (Grant No. 21QYCX0016), National Flash Flood Investigation and Evaluation Project (Grant No. SHZH-IWHR-57), National Key R&D Program of China (2020YFD1100701), and the Science and Technology Project of Xizang Autonomous Region (Grant No. XZ201901-GA-07), Project form Science and Technology Bureau of Altay Region in Yili Kazak Autonomous Prefecture.

Competing interests. The authors declare that they have no known competing financial interests or personal relationships that could have appeared to influence the work reported in this paper.

Availability of data and material. The population data are available at https://www. worldpop.org/ (last access: April 2019). The land use data are available at https:// ladsweb.modaps.eosdis.nasa.gov/ (last

access: September 2019). The GDP data are available at https://datadryad.org/stash/dataset /doi:10.5061/dryad.dk1j0 (last access: October 2019). The data connected with infrastructure, including data from hospitals, shelters, and road density data are available at https://www.openstreetmap.org/ (last access: December 2019). The digital elevation model (DEM) data are available at http://srtm.csi.cgiar.org/srtmdata/ (last access: September 2018). The impervious surface data are available at https://ghslsys.jrc.ec.europa.eu/ (last access: December 2019).

Code availability. Not applicable

Author contributions. YD, YL, and YFH were responsible for the collection and processing of the dataset. YD and JNX conceptualized the study and developed the methodology. YD and JNX were responsible for the analysis and validation of the results, and finished the original draft preparation. YD, JNX, WMC, NW, JL, WH, GY all participated in the reviewing of methodology, results, and article. All authors contributed to paper preparation and agreed to the published version of the manuscript.

1. Introduction

Floods rank among the most serious natural disasters in the world. Currently, floods tend to occur more frequently than other disasters, including earthquakes, forest fires, typhoons, heavy snows, and droughts (He Y-Y, Zhou J-Z, Kou P-G, Lu N, & Zou Q 2011; Njock PGA, Shen S-L, Zhou A-N, & Lyu H-M 2020). According to recent estimates, the economic losses caused by floods account for 40% of the

84 total losses caused by all natural disasters (Xia F-Q, Kang X-W, Wu S-H, Yang Q-Y, Ma X, Yang P-G,
85 & Li X-D 2008). Several studies have indicated that frequent flood events have led to a worldwide
86 increase in flood risk (Hu P, Zhang Q, Shi P-J, Chen B, & Fang J-Y 2018; Lyu H-M, Shen S-L, Yang J,
87 & Yin Z-Y 2019; Lyu H-M, Shen S-L, Zhou A-N, & Yang J 2020; Lyu H-M, Shen S-L, Zhou A-N, &
88 Zhou W-H 2019; Werren G, Reynard E, Lane SN, & Balin D 2016; Wu J, Yang R, & Song J 2018). Based
89 on the statistics from the Emergency Disasters Database (EM-DAT, CRED, http://www.emdat. be/), in
90 the Belt and Road region, 1,483 floods occurred from 2000 to 2020 here, accounting for 44.9% of the
91 total floods around the world. However, most of the countries along the Belt and Road region are
92 developing countries with underdeveloped economies and weak disaster resilience that lack the material
93 reserves and emergency relief capabilities needed to respond to disasters (Cui P, Wu S-N, Lei Y, Zhang
94 Z-T, & Zou Q 2020). According to the EM-DAT, the disaster losses in the developing countries along the
95 Belt and Road are more than twice the global average, and the death rate of people due to disasters is
96 much higher than the global average (Ge Y-G, Cui P, & Chen X-Q 2020). For example, between 2011
97 and 2013, the Philippines suffered recurrent floods that caused more than 100 fatalities per year, while
98 India and Nepal recorded 6,648 flood fatalities in 2013. Additionally, frequent floods are a major threat
99 to investment and engineering safety and regional development in the Belt and Road region (Ge Y-G,
100 Cui P, & Chen X-Q 2020). More seriously, under future climate change scenarios, the incidence and
101 intensity of flood disasters are likely to increase significantly (Chen H-L, Ito Y, Sawamukai M, &
102 Tokunaga T 2015; Fang Y, Yin J, & Wu B-H 2016; Jongman B, Ward PJ, & Aerts JCJH 2012; Ntajal J,
103 Lamptey BL, Mahamadou IB, & Nyarko BK 2017). In this sense, it is of paramount importance and
104 necessity to establish a scientific basis for flood prevention and mitigation in the Belt and Road region.

Vulnerability studies are currently gaining momentum, and the concept of vulnerability has been widely used in many fields and disciplines, as well as at different spatial levels. Yet, this term varies by discipline and research field (Fraser EDG, Dougill AJ, Mabee WE, Reed M, & Mcalpine P 2006; Janssen MA, Schoon ML, Ke W, & Börner K 2006; Liverman D and O'Brien K 1991; Metzger MJ, Rounsevell MDA, Acosta-Michlik L, Leemans R, & Schröter D 2006). In recent decades, our understanding of flood vulnerability has improved due to the use of combined indicators, case studies and analogues, stakeholder-driven processes, and scenario construction methods (Fekete A 2012; Malone EL and Engle NL 2011). Currently, in flood studies, vulnerability is most often conceptualized as a component that consists of exposure to disturbance or external stress, sensitivity to disturbance, and the capability to adapt or the coping capacity (Adger WN 2006; Weis SWM, Agostini VN, Roth LM, Gilmer B, Schill SR, Knowles JE, & Blyther R 2016; Zhou S-E, Zhang M-J, & Wang S-J 2018). Additionally, previous studies have shown that flood vulnerability is positively correlated with exposure and is negatively correlated with the disaster reduction capability (Rawat PK, Pant CC, Tiwari PC, & Sharma PDPK 2012). Throughout history, the disaster reduction capability has primarily included susceptibility, resilience, and coping capacity (Bodoque JM, Amerigo M, Díez-Herrero A, García JA, Cortés B, Ballesteros-Cánovas JA, & Olcina J 2016; Ding M-T, Heiser M, Hubl J, & Fuchs S 2016; Gallopín G 2006; Spitalar M, Gourley JJ, Lutoff C, Kirstetter PE, Brilly M, & Carr N 2014; Xiong J-N, Li J, Cheng W-M, Wang N, & Guo L 2019). Although the concept of the disaster reduction capability varies according to different authors, in this study, it consists of the susceptibility and coping capacity. In this study, susceptibility and coping capacity are both a measure of the physical and social nature of the carrier. Thus, a vulnerability assessment model that consists of the social exposure, susceptibility, and coping capacity was developed.

The four main types of methods that have been used to assess flood vulnerability include (1) the historical data-based approach (Adikari Y, Osti R, & Noro T 2010; Shi Y, Xu S-Y, & Shi C 2011), (2) the scenario simulation method (Li Z-H, Nadim F, Huang H-W, Uzielli M, & Lacasse S 2010; Shi Y 2013), (3) the vulnerability curve method (Zong N 2013), and (4) the index-based system (Ding M-T, Heiser M, Hubl J, & Fuchs S 2016; Hoque MA, Tasfia S, Ahmed N, & Pradhan B 2019). The historical data-based approach responds to the combined effects of the natural and social vulnerability and is highly practical for vulnerability distillation. However, it is directly influenced by the level of informativeness of the disaster documentation (Lyu H-M, Zhou W-H, Shen S-L, & Zhou A-N 2020). Scenario simulation methods are based on scenario models, which are quantitative predictions. Scenario-based vulnerability analysis is typically used to predict flood vulnerability in small areas, and the application of this method is limited by the fact that floods usually occur at the regional scale (Sampson CC, Fewtrell TJ, Duncan A, Shaad K, Horritt MS, & Bates PD 2012). As for the vulnerability curve method, it primarily focuses on assessing the relationship between the intensity of a range of hazards and the degree to which various hazard-bearing individuals are affected (Shi Y 2013). However, this method requires field statistics and questionnaires, and therefore, it is not suitable for replication and implementation on a large scale. Among these four methods, the index-based system is the most widely applied method in flood vulnerability assessment (Zhang Z-G 2014). Notably, the index-based system has the advantages of easy access to data, simple modeling and calculations, and the ability to reflect the regional vulnerability situation at a macroscopic level. Thus, the index-based system was applied in this study. To quantify the indexes more precisely, quantitative research has progressed from the investigation of a single method to that of multiple methods. Generally, these methods include multiple-criteria decision making (MCDM)

methods (Lyu H-M, Zhou W-H, Shen S-L, & Zhou A-N 2020) and machine learning methods (Xiong J-N, Sun M, Zhang H, Cheng W-M, Yang Y-H, Sun M-Y, Cao Y-F et al. 2019). Among the MCDM methods, the triangular fuzzy number-based analytic hierarchy process (TFN-AHP) is one of the most widely used and mature approaches (Lyu H-M, Zhou W-H, Shen S-L, & Zhou A-N 2020). Additionally, compared with other machine learning methods, the support vector machine (SVM) is a supervised machine learning technique based on statistical learning theory and the principle of structural risk minimization. The SVM not only avoids the effects of human factors, but it also expands the amount of information. Thus, in this study, the TFN-AHP and SVM were used as the quantification methods for the index-based system.

However, the knowledge base regarding large-scale flood risk and vulnerability is quite limited (Jongman B, Ward PJ, & Aerts JCJH 2012). Traditionally, flood vulnerability assessments have been limited to national (de Moel H and Aerts JCJH 2011; Xiong J-N, Li J, Cheng W-M, Wang N, & Guo L 2019) and even regional scales (Bouwer LM, Bubeck P, & Aerts JCJH 2010; Lyu H-M, Zhou W-H, Shen S-L, & Zhou A-N 2020). Based on the physical and social aspects, some scholars have conducted temporal and spatial analyses of the vulnerability of flood disasters in the United States (Cutter SL and Finch C 2008; Spitalar M, Gourley JJ, Lutoff C, Kirstetter PE, Brilly M, & Carr N 2014). They concluded that indicator-based vulnerability assessments are a key factor in emergency preparedness, disaster mitigation planning, immediate responses, and long-term disaster recovery. At the regional scale, many studies have focused on quantitative methods of vulnerability assessments. This differs from the statistical analyses applied at the national scale. For instance, Ding et al. selected 13 index factors that included economic density, population density, building density and farmland coverage, road density,

and GDP per capita to conduct an assessment of the debris flow vulnerability in the upper reaches of the Min River (Ding M-T, Heiser M, Hubl J, & Fuchs S 2016). In addition, Lyu et al. applied AHP and TFN-AHP in an inundation risk assessment of the metro system in Shenzhen (Lyu H-M, Zhou W-H, Shen S-L, & Zhou A-N 2020). Their results showed that the TFN-AHP had a higher accuracy than AHP. Obviously, previous studies have shown that the indicator-based system is currently the dominant flood vulnerability evaluation method. However, the application of the methodologies and data used in regional studies has been difficult to apply at larger scales (Hu P, Zhang Q, Shi P-J, Chen B, & Fang J-Y 2018; Jongman B, Ward PJ, & Aerts JCJH 2012). In particular, most countries along the Belt and Road region are so underdeveloped and developing that they lack information sharing and international disaster reduction cooperation mechanisms, resulting in many of their fundamental data being inaccurate (Ge Y-G, Cui P, & Chen X-Q 2020). Thus, research regarding the flood vulnerability in the Belt and Road region requires more in-depth investigations because this region has experienced increasing climate extremes in recent years, and the area is extremely vulnerable to flood disasters (Komolafe AA, Herath S, & Avtar R 2019; Lugeri N, Kundzewicz ZW, Genovese E, Hochrainer S, & Radziejewski M 2010; Sam AS, Kumar R, Kachele H, & Muller K 2017).

Given these problems, in this study, a flood vulnerability assessment based on the need for flood disaster prevention and mitigation throughout the Belt and Road Region was conducted. The primary objectives of this study are as follows. (1) Establish an index system for evaluating the vulnerability of flood disasters throughout the Belt and Road region, including exposure and disaster reduction capability. (2) Build a new vulnerability assessment model for large-scale studies based on the triangular fuzzy number-based analytic hierarchy process (TFN-AHP) and support vector machine (SVM) to obtain the

results of flood vulnerability assessment throughout the Belt and Road region. (3) Map and analyze the spatial characteristics of the flood exposure, disaster reduction capability, and vulnerability based on the assessment results.

2. Materials

2.1. Study area

The Belt and Road region (approximately 50,640,400 km^2) consists of 65 countries across the Asian, European, and African continents. It contains approximately 4.4 billion people and has a combined GDP of 2.3 billion dollars, accounting for 63% and 29% of the world totals, respectively (Zhang J-D 2018). As shown in Fig. 1, this region has an undulating terrain. The highest altitude is greater than 8500 m, while the lowest altitude is less than 0 m. In addition, this region is dominated by eight types of climate, including both monsoons and continental climate characteristics, and the regional distribution of water resources is uneven (Zhou J, Jiang T, Wang Y-J, Su B-D, & Zhai J-Q 2020). In terms of precipitation, the average annual total precipitation from 2000 to 2018 increased from 0.92 mm in the northwest to 6,067.71 mm in the southeast in this area. Due to the diverse natural environments, the types of terrains, and the uneven distribution of precipitation, natural disasters, especially droughts and floods, occur frequently in this area. According to the incomplete statistics from the Emergency Disasters Database (EM-DAT, CRED, http://www.emdat.be/), 1561 floods have occurred throughout the Belt and Road Region since the beginning of the 21st century, while the number of floods from 1975 to 2000 was only 700 (Hu P, Zhang Q, Shi P-J, Chen B, & Fang J-Y 2018).

2.2. Datasets and sources

In this study, data related to the flood vulnerability were classified into four aspects: (1) The data related to society and the economy, including population data, land use data, and GDP data. These data were obtained from the World Pop (https://www.worldpop.org/), the National Aeronautics and Space Administration, NASA (https://ladsweb.modaps.eosdis.nasa.gov/), and the Dryad (https://datadryad.org/stash/dataset/doi:10.5061/dryad.dk1j0). Notably, the GDP data on the Dryad was come from the Gridded global datasets for Gross Domestic Product and Human Development Index over 1990-2015 (Kummu M, Taka M, & Guillaume JHA 2018). (2) The data connected with infrastructure, including data from hospitals, shelters, and road density data were downloaded from OpenStreetMap (https://www.openstreetmap.org/). (3) The digital elevation model (DEM) data were obtained from the Shuttle Radar Topography Mission (SRTM) data (http://srtm.csi. cgiar.org/srtmdata/). (4) The impervious surface data were collected from the Global Human Settlement Layer, GHSL (https://ghslsys.jrc.ec.europa.eu/). Table 1 presents the characteristics of the datasets used in this study.

2.3. Establishing the assessment index system

2.3.1. Assessment unit

Generally, the results of the assessment are directly affected by the size and boundary of the assessment units, which are the fundamental elements of a vulnerability assessment (Cascini L 2008; Li L-T, Xu Z-X, Pang B, & Liu L 2012). The assessment units that previous studies have commonly used include regional units, grid units, slope units, topographic units, and uniform condition units (Liu X-L, Cheng M, & Tian C-S 2017; Zhou Y, Li N, Wu W-X, & Wu J-D 2014). In this study, the exposure

assessment indexes (population density, economic density, building density, and farmland density) were expressed completely as raster maps. In addition, the assessment indexes of the disaster reduction capability (hospital density, shelter density and road density) were expressed as vector maps. The other indexes (impervious surface, the dependent population, female population, and GDP per capita) were expressed in raster format. In order to make a more detailed analysis of all of these indexes, the total study area was divided into 646,191 grid cells with a spatial resolution of 0.1° ×0.1° .

2.3.2. Index system

After confirming the assessment unit used for this study, the assessment index system was established. Notably, the establishment of an assessment index system is a key step in building a flood vulnerability assessment. This index system was established after summarizing the results of previous studies to define the vulnerability (Ding M-T, Heiser M, Hubl J, & Fuchs S 2016; Weis SWM, Agostini VN, Roth LM, Gilmer B, Schill SR, Knowles JE, & Blyther R 2016; Xiong J-N, Li J, Cheng W-M, Wang N, & Guo L 2019). In the numerous previous studies reviewed, vulnerability was most commonly conceptualized as a component consisting of exposure to a disturbance or external stress, sensitivity to a disturbance, and the capability to adapt (Adger WN 2006; Gallopín G 2006). In this study, the disaster reduction capability was regarded as a combination of the susceptibility and coping capacity. Therefore, the vulnerability to floods was divided into two portions: the exposure and disaster reduction capability. The exposure indexes consist of population density, economic density, building density, and farmland density. The disaster reduction capability indexes include impervious surface, dependent population, female population, hospital density, shelter density, road density, and GDP per capita. As shown in Fig.

2, eleven assessment indexes were selected in this study.

3. Methodology

3.1. Exposure assessment

3.1.1. Calculation of the exposure indexes

According to previous studies, in areas with higher exposure, the higher the vulnerability, the greater the losses a flood will cause. Recently, several studies have divided vulnerability into two parts: physical vulnerability and social vulnerability (Erena SH and Worku H 2019; Hoque MA, Tasfia S, Ahmed N, & Pradhan B 2019), however, other studies have only analyzed one level, the physical or social level (Rani NNVS, Satyanarayana ANV, & Bhaskaran PK 2015; Rimba AB, Setiawati MD, Sambah AB, & Miura F 2017; Susan L and Cutter 2003; Zhang Y-L and You W-J 2014). In this study, the primary focus was the social level. Additionally, the comprehensive impact of hazards and disasters on the environment was regarded as a threat or danger; while exposed units, such as real estate, farmland, and a human presence, were regarded as characteristics of the regional socioeconomic system (Huang J-Y, Liu Y, & Ma L 2011). Thus, in this study, the population density, economic density, building density, and farmland density were used to calculate the social exposure. To some extent, because the exposure factors were measured at different scales, certain reclassifications were necessary to convert the exposure factors into five comparable units or exposure classes: 5 (extremely high exposure), 4 (high exposure), 3 (moderate exposure), 2 (low exposure), and 1 (extremely low exposure) (Mahmoud SH and Gan TY 2018). The specific indicators of exposure were defined as follows:

(1) Population density

Population is directly related to flood disasters, and the consequences of flood disasters are also larger in densely populated areas. In this study, the population density represents the population per assessment unit ($D = P_i/S_i$), where D is the population density; P_i is the population of region i; and S_i represents the area of region i.

(2) Economic density

In this study, economic density refers to the GDP per assessment unit ($D = G_i/S_i$), where D is the economic density; G_i is the GDP of region i; and S_i represents the area of region i. Proverbially, the GDP is closely connected to flood disasters, and in most cases, regions with higher GDP have stronger disaster adaptation capacity, but the consequences of a flood disaster are also likely to be greater in these regions.

(3) Building density

Building density refers to the building area per assessment unit ($D = B_i/S_i$), where D is the building density; B_i represents the number of buildings in region i; and S_i is the area of region i. Here, the density of buildings was reflected using the ratio of the building area to the Belt and Road region, while neglecting the different heights of the buildings.

(4) Farmland density

The farmland density refers to the farmland area per assessment unit ($D = F_i/S_i$), where D is the farmland density, F_i represents the amount of farmland in region i; and S_i is the area of region i. In this study, the building density and farmland density factors were both extracted from the land use data, and they indicate the importance of local construction and agricultural activities, respectively.

3.1.2. Triangular fuzzy number-based AHP

In this study, the triangular fuzzy number-based analytic hierarchy process (TFN-AHP) was used to calculate the exposure. In the application of the traditional AHP, since the pair comparison is based on the opinions of the decision makers, the value that represents the relative importance is subjective. The bias caused by this subjective importance leads to uncertainty in the evaluation weight. In comparison, the TFN-AHP is based on the application of a triangular fuzzy number in the traditional AHP, which can reduce the impact of this uncertainty (Lyu H-M, Shen S-L, Yang J, & Yin Z-Y 2019). Instead of the definite number the AHP uses, in the TFN-AHP, a triangular fuzzy number is used to reveal the degrees of importance of the evaluation factors. In the application of the TFN-AHP, the triangular fuzzy number is defined as P, and it can be calculated as follows:

$$P = (l, m, \mu)\ (l \le m \le \mu) \tag{1}$$

where P is the triangular fuzzy number; m is the most likely value; and l and μ are the minimal and maximum values, respectively. From this we can see the most probable value for m is jointly determined by the parameters l and μ. The meaning of the triangular fuzzy number and the detailed methods of the parameter calculation have been discussed in previous studies (Lyu H-M, Shen S-L, Yang J, & Yin Z-Y 2019; Zhang Y-L and You W-J 2014). In this study, the TFN-AHP was used to confirm the relative significance of each pair of factors using a 9-point system from 1 (equal importance) to 9 (extreme importance) (Table 2).

In the application of the TFN-AHP, the triangular fuzzy numbers were used in the judgment matrix. Notably, it is of vital importance to construct the triangular fuzzy judgment matrix used in the TFN-AHP.

The Eq. (2) shows a fuzzy judgment matrix of the triangular fuzzy numbers. According to the normalized indexes of the exposure assessment, the corresponding weights of these indexes were calculated using the TFN-AHP, as shown in Table 3.

$$\begin{pmatrix} [1,\ 1,\ 1] & [l_{12}, m_{12}, \mu_{12}] & \mathrm{L} & [l_{1i}, m_{1i}, \mu_{1i}] & \mathrm{L} & [l_{1n}, m_{1n}, \mu_{1n}] \\ \left[\frac{1}{\mu_{12}}, \frac{1}{m_{12}}, \frac{1}{l_{12}}\right] & [1,\ 1,\ 1] & \mathrm{L} & [l_{2i}, m_{2i}, \mu_{2i}] & \mathrm{L} & [l_{2n}, m_{2n}, \mu_{2n}] \\ \mathrm{L} & \mathrm{L} & \mathrm{O} & \mathrm{L} & \mathrm{L} & \mathrm{L} \\ \left[\frac{1}{\mu_{1i}}, \frac{1}{m_{1i}}, \frac{1}{l_{1i}}\right] & \left[\frac{1}{\mu_{2i}}, \frac{1}{m_{2i}}, \frac{1}{l_{2i}}\right] & \mathrm{L} & [1,\ 1,\ 1] & \mathrm{L} & [l_{in}, m_{in}, \mu_{in}] \\ \mathrm{L} & \mathrm{L} & \mathrm{O} & \mathrm{L} & \mathrm{L} & \mathrm{L} \\ \left[\frac{1}{\mu_{1n}}, \frac{1}{m_{1n}}, \frac{1}{l_{1n}}\right] & \left[\frac{1}{\mu_{2n}}, \frac{1}{m_{2n}}, \frac{1}{l_{2n}}\right] & \mathrm{L} & \left[\frac{1}{\mu_{in}}, \frac{1}{m_{in}}, \frac{1}{l_{in}}\right] & \mathrm{L} & [1,\ 1,\ 1] \end{pmatrix} \quad (2)$$

3.2. Disaster reduction capability assessment

3.2.1. Calculation of the disaster reduction capability indexes

Previous studies have suggested that the higher capability of the disaster reduction capability is, the lower the losses caused by flood disasters will be. In a general sense, susceptibility is the degree or the depth to which a disaster-bearing body or system is affected by a disaster of the same intensity. Numerous studies have suggested that not all individuals and groups exposed to a hazard are equally susceptible (Hoque MA, Tasfia S, Ahmed N, & Pradhan B 2019; Huang J-Y, Liu Y, & Ma L 2011; Liu J and Wang S-Y 2013). Therefore, data of the impervious surface, dependent populations, and female populations were collected as susceptibility factors. In this study, the coping capability primarily relies on the capability of people, organizations and systems to manage the effects of disasters using the available skills and resources (Rana IA and Routray JK 2018). At this level, four coping capability criteria,

namely, the hospital density, shelter density, road density and GDP per capita, were selected here. The specific indicators of the disaster reduction capacity of flood disasters were selected as follows:

1 Susceptibility

(1) Impervious surface

Urbanization has an adverse impact on the environment, especially when the urban growth rate and the carrying capacity do not co-evolve, including the management capacity, natural resources, and basic service provisions (Lee S, Okazumi T, Kwak Y, & Takeuchi K 2015). One of the effects of urbanization is an increase in impervious surface, which makes peak discharges intense and rapid.

(2) Dependent population

In certain previous studies, children (0-15 years old) and the elderly (people over 65) were considered to be dependent people, who often need support from other groups when floods are occurring (Li L-T, Xu Z-X, Pang B, & Liu L 2012; Sharma SVS, Roy PS, Chakravarthi V, & Rao GS 2017). To some extent, children and the elderly often have less access to information and more difficulty in taking personal actions to prepare for floods. In this study, the index of the dependent population was produced using 2015 population data.

(3) Female population

Females are affected by floods in numerous ways due to their limited mobility and difficulty in evacuation during emergency cases (Eric N and Thomas P 2007; Hoque MA, Tasfia S, Ahmed N, & Pradhan B 2019). Generally speaking, the female population is more vulnerable than the male population.

2 Coping capacity

(1) Hospital density

The hospitals in this study refer to large hospitals in modern cities, not those in small regions. Proverbially, the higher the hospital density in a city, the higher the capacity of the people coping with floods and recovering from flood disasters. Moreover, the hospital density refers to the number of hospitals per assessment unit ($D = H_i/S_i$), where D is the hospital density; H_i is the number of hospitals in region i; and S_i represents the area of region i.

(2) Shelter density

In this study, shelters were defined as the emergency shelters where people can take refuge from flood disasters. The shelter density refers to the number of shelters in an assessment unit ($D = Sh_i/S_i$), where D is the shelter density; Sh_i is the number of shelters in a region i; and S_i denotes the area of region i.

(3) Road density

Here, roads primarily refer to freeways, provincial, and national highways. It is assumed that the higher the road density is, the higher the capacity of the people coping with floods will be. Road density refers to the total length of all types of roads in per an assessment unit ($D = R_i/S_i$), where D is the road density; R_i is the total length of all roads in region i; and S_i represents the area of region i.

(4) GDP per capita

The GDP per capita was used to evaluate the economic development level of a grid unit. Accordingly, the GDP per capita is a better indicator of the status, rate, and level of economic

development. Generally speaking, the higher the GDP per capita is, the stronger the coping capacity of a region. In this study, the GDP per capita data were calculated by dividing the GDP data by the population data.

3.2.2. Support vector machine

In this study, initially the weights in the indexes of the disaster reduction capability were not clear, and thus, the support vector machine (SVM) was used to calculate the disaster reduction capability. The SVM is a new method developed in recent years that is based on a nonlinear transformation, and it is widely used in flood risk assessment (Xian S-D 2010). Notably, the SVM is also a supervised learning binary classifier that is based on the structural risk minimization principle (Wan SA and Lei TC 2009; Yao X, Tham LG, & Dai F-C 2008), and it can also explore the hidden relationships between inputs and outputs (Xu C, Dai F-C, Xu X-W, & Lee YH 2012). The mechanism of a flood vulnerability assessment is complex due to the effects of incomplete information and the numerous uncertainties. To reduce the impact of these uncertainties, the SVM model was used to calculate the internal rules based on many complex fuzzy input and output variables. The primary steps of the algorithm are as follows:

(1) Assume a training set of a known sample set is $T = \{x_1, x_2, \ldots, x_n, y\}$, where x_i is the ith input data $x_i \in R_n$, and y is the output data, $i = 1, 2, \ldots, n$.

(2) Then, all of the data are classified into two categories, and n-dimensional hyperplanes are used to obtain the maximum interval. This is demonstrated in Eq. (3) and (4).

$$\frac{1}{2}\|w\|^2 \tag{3}$$

$$\text{Subject to } y_i((w \cdot x_i) + b) \geq 1 \tag{4}$$

where ||*w*|| represents the norm of the hyperplane normal; *b* denotes a scale base; and (••) is the scalar product operation.

(3) With the use of the Lagrange multiplier, the definition of the cost function is as follows:

$$L = \frac{1}{2}\|w\|^2 - \sum_{i=1}^{n} \lambda_i (y_i((w \cdot x_i) + b) - 1) \quad (5)$$

where λ_i is the Lagrange multiplier. The solution can be obtained by using the dual minimization of Eq. (6) with *w* and *b* (Cherkassky V 1997).

(4) For inseparable situations, the constraint conditions can be modified by introducing slack variables, ξ_i (Cherkassky V 1997):

$$y_i((w \cdot x_i) + b) \geq 1 - \xi_i \quad (6)$$

Therefore, Eq. (7) becomes

$$L = \frac{1}{2}\|w\|^2 - \frac{1}{vn}\sum_{i=1}^{n} \xi_i \quad (7)$$

where $v \in$ (0,1], which is introduced to explain the misclassification (Franklin J 2005; Xu C, Dai F-C, Xu X-W, & Lee YH 2012).

In this study, a kernel function, $K(x_i, x_j)$, was used to make the nonlinear decision boundary clear (Cherkassky V 1997). In recent studies, the linear kernel (LN), the polynomial kernel (PL), the sigmoid kernel (SIG), and the radial basis function kernel (RBF) are the kernel types most used for SVM analysis. The RBF was used in this study:

$$K(x_i, x_j) = e^{-\gamma(x_i - x_j)^2}, \gamma > 0 \quad (8)$$

where γ is a parameter of the kernel function.

3.3. Vulnerability assessment

Previous studies have verified that flood vulnerability is positively correlated with the degree of exposure and is negatively correlated with the disaster reduction capability (Ding M-T, Heiser M, Hubl J, & Fuchs S 2016; Rawat PK, Pant CC, Tiwari PC, & Sharma PDPK 2012). Thus, the vulnerability was calculated using various data types as proxies for the exposure and disaster reduction capability. Based on several previous studies (Ding M-T, Heiser M, Hubl J, & Fuchs S 2016; Liu X-L and Lei J-Z 2003; Xiong J-N, Li J, Cheng W-M, Wang N, & Guo L 2019), the vulnerability model was applied using Eq. (9). In this study, using the natural break point method, the results of the exposure, the disaster reduction capability, and the vulnerability were divided into five levels: very low, low, moderate, high, and extremely high (Hoque MA, Tasfia S, Ahmed N, & Pradhan B 2019; Tehrany MS, Pradhan B, & Jebur MN 2013; 2014).

$$V = E(1-\sqrt{Re}) \tag{9}$$

where V is the vulnerability; E is the exposure; and Re is the disaster reduction capability.

3.4. Assessment procedure

As indicated in Fig. 3, the flowchart consists of three major phases. First, the data that were collected from several different websites were preprocessed. The primary step in this phase was normalizing the data and inputting these data into the grids. Subsequently, in the second phase, the data were divided into two aspects: the exposure index and the disaster reduction capability index. After that, the weights of the exposure factors were calculated using the TFN-AHP based on ArcGIS 10.6. As for the calculation of the disaster reduction capability, the factors were input into the support vector machine

using the R software. In the third phase, based on the vulnerability obtained using Eq. (9), the results of the flood vulnerability were mapped, and a spatial analysis was conducted.

4. Results

4.1. Exposure assessment

In this study, in order to intuitively quantify the results, the results of the exposure were placed into 646,191 grid cells. As is illustrated Table 4, the statistical results of each level of the quantity, area, and proportion in the exposure assessment can be seen. It was discovered that most of the regions (43,781,500 km^2) have extremely low exposure, accounting for approximately 86% of the total area. The area of the low exposure regions is 3,446,200 km^2, which is larger than the entire area of India. Furthermore, 25,977 grid cells (2,035,700 km^2) have moderate exposure, 13,053 grid cells (1,021,100 km^2) have high exposure, and 4523 grid cells (355,900 km^2) have extremely high exposure, accounting for approximately 0.70%.

As shown in Fig. 4, a map of the flood exposure throughout the Belt and Road region was produced. It can be seen that most of the areas have extremely low and low exposure. However, in this analysis, our attention was focused more on those areas with higher exposure, which are likely to suffer more economic and population losses when floods occur. In summary, Fig. 4 shows that the higher exposure areas are primarily located in the eastern and southern parts of Asia, including eastern China, northern India, the Indus Valley in Pakistan, the central region of Indonesia, and most of Bangladesh. Locally, the extremely high exposure areas are primarily distributed in the capitals and major cities of the countries in the Belt and Road region, such as Beijing, Shanghai, Chengdu, New Delhi, Bangkok, Jakarta, Moscow,

Abu, Riyadh, Kyiv, Baghdad, and Cairo. Obviously, these areas of higher exposure are densely populated and economically developed. This is consistent with the larger proportions of the population density and economic density in the exposure indicators.

4.2. Disaster reduction capability assessment

The statistical results of each level of the quantity, area, and proportion of the disaster reduction capability are presents in Table 5. It was found that in most regions, the disaster reduction capability is extremely low (407,853,000 km^2) and low (7,869,200 km^2), accounting for 80.53% and 15.54% of the total area, respectively. The areas with moderate disaster reduction capability merely only account for 3.26%. Notably, the areas with high and extremely high disaster reduction capacity both account for less than 1% of the total area. There are only 3,683 grid cells (287,200 km^2) and 648 grid cells (49,300 km^2) with high and extremely high disaster reduction capability, accounting for 0.57% and 0.10%, respectively.

As for the spatial distribution patterns, Fig. 5 shows that more than half of the areas have low disaster reduction capability, which is consistent with the above results. The areas with moderate disaster reduction capability are primarily located in the western and eastern parts of the Belt and Road region. Among these areas, only a portion are distributed in eastern China, southern Nepal, the central region of Indonesia and the Cairo region of Egypt, and the vast majority are concentrated in most of the regions of Europe. Notably, there few areas have high disaster reduction capability. As shown in Fig. 5, these areas are mainly concentrated in the major cities in the Belt and Road region, such as Beijing, Shanghai, Hong Kong, Taipei, Bangkok, Jakarta, New Delhi, Riyadh, Abu Dhabi, Cairo, Moscow, and several major cities in Europe.

463 *4.3. Vulnerability assessment*

464 According to the assessment results of the exposure and disaster reduction capability, the
465 vulnerability of each grid cell was calculated using Eq. (9). The statistical results of each grade of the
466 quantity, area, and proportion of the vulnerability are presented in Table 6. As can be seen, vulnerability
467 of most regions (43,817,500 km^2) is extremely low, accounting for 86.53% of the total area. Furthermore,
468 41,938 grid cells (3,287,800 km^2) have low vulnerability, and 22,229 grid cells (1,744,200 km^2) have
469 moderate vulnerability. The areas with high and extremely high vulnerabilities, with disaster distribution
470 densities of 1,236,100 and 554,800 km^2, respectively, account for 2.36 and 1.19% of the total area,
471 respectively.

472 According to Eq. (9), the vulnerability to floods is positively related to the exposure and negatively
473 related to the disaster reduction capability. Similar to the distribution of the exposure, most areas have
474 low and extremely low vulnerability, occupying most of the proportion of the Belt and Road region (Fig.
475 6). In addition, the areas with high and extremely high vulnerability are primarily distributed in the
476 southern and eastern parts of China, northern India, most of Bangladesh, the Indus Valley in Pakistan,
477 the Nile River Basin in Egypt, the central region of Indonesia, and major cities in the Belt and Road
478 region. These highly vulnerable areas coincide with the areas characterized by frequent economic
479 activities and dense populations, such as eastern China and northern India, in particular. In contrast to
480 the positive correlation between the exposure and vulnerability, the disaster reduction capability
481 decreases the vulnerability to floods. Thus, those areas with higher disaster reduction capability have
482 lower-levels of vulnerability, such as Bangkok of Thailand, Kuala Lumpur of Malaysia, Riyadh in the

Kingdom of Saudi Arabia, the Kyiv of Ukraine, and Moscow in Russia.

5. Discussion

5.1. Assessment methodology

In this study, a multi-dimensional analysis of the indexes used to calculate the flood vulnerability throughout the Belt and Road region was proposed. Regarding the vulnerability to flood disasters, several previous studies have emphasized the importance of quantifying the exposure and disaster reduction capability (Kim ES and Choi HI 2011; Li Z-H, Nadim F, Huang H-W, Uzielli M, & Lacasse S 2010; Xiong J-N, Li J, Cheng W-M, Wang N, & Guo L 2019). Thus, the model was extended to a more comprehensive assessment of the flood vulnerability of the Belt and Road region, and it included social exposure, susceptibility, and coping capacity. Based on the index-based system, we conducted a flood vulnerability assessment of the Belt and Road region. In vulnerability assessments, the AHP is one of the most commonly used weighting methods. By applying the AHP, all of the factors are compared in pairs based on the opinions of the decision makers. However, the final weight obtained is a certain number, causing the resulting values to represent their relative importance, which is subjective (Mahmoud SH and Gan TY 2018). Compared with the AHP, the TFN-based weight is a triangular fuzzy number, not a definite number, which can reduce the impact of these subjectivities on the vulnerability assessment (Lyu H-M, Zhou W-H, Shen S-L, & Zhou A-N 2020). In the application of the TFN-AHP, the median value of the triangular fuzzy number denotes the largest probability of the evaluation model, while the minimum and maximum values represent the ambiguity corresponding to the largest probability (Cheng Z-L, Zhou W-H, & Garg A 2020; Lyu H-M, Shen S-L, Zhou A-N, & Yang J 2020; Lyu H-M, Shen S-L,

503 Zhou A-N, & Zhou W-H 2019; Yang X-L, Ding J-H, & Hou H 2013). Although the TFN-AHP using the
504 fuzzy theory can reduce the subjective influence of an artificial weight determination, it cannot perform
505 completely objectively in the vulnerability assessment. Additionally, the weights of some of the indexes
506 of the disaster reduction capability were not clear, and therefore, the SVM model was used to calculate
507 the disaster reduction capability. In addition to the characteristics of the general machine learning
508 methods, the SVM model is a supervised machine learning technique based on statistical learning theory
509 and the principle of structural risk minimization (Bui DT, Pradhan B, Lofman O, & Revhaug I 2012;
510 Tehrany MS, Pradhan B, & Jebur MN 2014; Tehrany MS, Pradhan B, Mansor S, & Ahmad N 2015; Yao
511 X, Tham LG, & Dai F-C 2008). Currently, the SVM is widely used in flood disaster assessment studies.
512 Compared with previous models, the support vector machine (SVM) method not only avoids the effects
513 of human factors, but it also expands the amount of information (Xiong J-N, Li J, Cheng W-M, Wang N,
514 & Guo L 2019).

515 *5.2. The spatial patterns of the exposure, the disaster reduction capability, and the vulnerability to floods.*

516 In this study, the results indicate that the vulnerability is positively related to exposure and is
517 negatively correlated with the disaster reduction capability, which is consistent with the results of
518 previous studies (Ding M-T, Heiser M, Hubl J, & Fuchs S 2016; Xiong J-N, Li J, Cheng W-M, Wang N,
519 & Guo L 2019). In fact, there is no vulnerability when the exposure is equal to 0 because “a hazard is not
520 hazardous unless it threatens something; [and] vulnerability does not exist unless some elements at risk
521 are threatened by something”(Ding M-T, Heiser M, Hubl J, & Fuchs S 2016). During the assessment
522 procedure, the weights of the assessment indexes have an important influence on the assessment result.

Notably, the population density and economic density are key indexes of exposure, while the other indexes are less important (Table 3) (Ding M-T, Heiser M, Hubl J, & Fuchs S 2016). As shown in Fig. 4, the spatial pattern of the exposure shows that areas with higher population density and higher GDP have a higher exposure to flood disasters (Ding M-T, Heiser M, Hubl J, & Fuchs S 2016; Hoque MA, Tasfia S, Ahmed N, & Pradhan B 2019; Tanoue M, Hirabayashi Y, & Ikeuchi H 2016). For instance, in the eastern parts of China, northern India, and the central region of Indonesia, due to the impact of their dense populations and high economic densities (An Y, Tan X-C, Gu B-H, & Zhu K-W ; Cui P, Wu S-N, Lei Y, Zhang Z-T, & Zou Q 2020), the exposure of these regions is relatively higher. In contrast to other areas, numerous capitals and major cities of these countries along the Belt and Road region have higher exposure, for example, Beijing, Shanghai, Guangzhou, Chengdu, Taipei, Hanoi, Manila, Bangkok, Bandung, New Delhi, Kolkata, Dhaka, Moscow, Cairo, and Abu Dhabi (Fig. 4). This is because capitals are often the political, economic, and cultural centers of their countries. In contrast, the exposure of most of the areas of the Belt and Road region is low and extremely low (Fig. 4), accounting for approximately 47,227,700 km^2 totally (Table 4). The reason for this phenomenon is that the maximum and minimum values of these indicators vary too much, although all of the exposure indicators were normalized and reclassified.

With respect to the disaster reduction capability, our findings indicate that the disaster reduction capability of most areas of the Belt and Road region is low, which is corresponds to the results of Ge (Ge Y-G, Cui P, & Chen X-Q 2020) and Cui (Cui P, Wu S-N, Lei Y, Zhang Z-T, & Zou Q 2020), who also demonstrated the weak disaster prevention and mitigation capabilities throughout the Belt and Road region. As shown in Fig. 5, most of the areas of the Belt and Road have extremely low (40,785,300 km^2)

544 and low (7,869,200 km^2) disaster reduction capability, accounting for 80.53% and 15.54% of the total
545 area, respectively (Table 5). Notably, most of the countries in this region have underdeveloped economies,
546 low levels of education, and high population densities, which leads to their overall disaster prevention
547 and resilience capabilities being weak (Cui P, Wu S-N, Lei Y, Zhang Z-T, & Zou Q 2020). In contrast,
548 the more developed cities and regions have higher disaster reduction capability, such as Beijing, Shanghai,
549 Chengdu, Guangzhou, Taipei, Hanoi, Bangkok, Kuala Lumpur, Dhaka, New Delhi, Moscow and Abu
550 Dhabi. Regionally, the areas with higher disaster reduction capability are primarily distributed in the
551 European countries, while a small amount is located in eastern China, the central region of Indonesia,
552 the Cairo region of Egypt, and several cities in western Russia (Fig. 5). The people in these areas can
553 respond quickly to losses and have a strong resistance to flood disasters (Jongman B, Ward PJ, & Aerts
554 JCJH 2012; Okazawa Y, Yeh PJF, Kanae S, & Oki T 2011). In addition, the spatial patterns of the disaster
555 reduction capability reveal that the areas with high hospital densities, high shelter densities, high road
556 densities and high GDP per capita have a lower incidence of flood disasters (Hoque MA, Tasfia S, Ahmed
557 N, & Pradhan B 2019), especially in the European countries (Fig. 5).

558 The results presented here support some of the important findings of previous studies. Similar to
559 the observations reported in several studies (Liu J-F, Wang X-Q, Zhang B, Li J, Zhang J-Q, & Liu X-Q
560 2017; Liu Y-S, Yang Z-S, Huang Y-H, & Liu C-J 2018), the resulting vulnerability throughout the Belt
561 and Road region (Fig. 6) indicates that the distribution characteristics of the vulnerability are similar to
562 that of the population density and GDP. In general, the spatial distribution of the vulnerability (Fig. 6) is
563 similar to that of the exposure (Fig. 4), which is in agreement with Eq. (9). Compared to earlier models,
564 which calculate vulnerability through the direct addition of the exposure, susceptibility, and coping

capacity, the information used in the approach proposed in this study is expanded (Ding M-T, Heiser M, Hubl J, & Fuchs S 2016). As can be seen Fig. 6, the vulnerability of most of the regions (43,817,500 km^2) is extremely low, accounting for 86.53% of the total area. Regionally, those areas with extremely high vulnerability are primarily distributed in eastern China, northern India, the Indus Valley in Pakistan, and most of Bangladesh, which are densely populated and economically concentrated. When these areas suffer from floods, the deaths and economic losses will be more severe than in other areas. Additionally, the level of vulnerability in many major cities (Fig. 6) is lower than that of the exposure (Fig. 4) due to their higher disaster reduction capabilities (Xiong J-N, Li J, Cheng W-M, Wang N, & Guo L 2019). As shown in Fig. 6, the typical regions and major cities are Bangkok, Kuala Lumpur, Bangalore, Cairo, Riyadh, Moscow, and Kyiv. Here, the response to floods mainly depends on the various flood defense structures. However, several studies have illustrated that there will be many difficulties in mitigating flood vulnerability if people only rely on flood defense structures. Methods, such as "living with rivers" and "making space for water", not only provide space for storing flood water, but also protect natural habitats (Johnson C, Penning-Rowsell E, & Tapsell S 2007). Future research should consider these aspects.

Overall, these results can help people understand which areas in the Belt and Road region are most threatened by flood disasters and which areas have better disaster reduction capabilities. Furthermore, these maps can help the governments of the countries in the Belt and Road region organize and project the future layout of populations, economies, cities, roads, and other infrastructure.

584 *5.3. Importance and limitations*

585 The United Nations Disaster Reduction Agency (UNISDR, 2011) recently stated that the exposure
586 of economies affected by floods is increasing in all regions of the world, while the risk of death in
587 developed countries is declining due to increased income and improved governance (such as emergency
588 planning and preparations) (Jongman B, Ward PJ, & Aerts JCJH 2012). However, most of the countries
589 in the Belt and Road region are developing countries, and their disaster prevention and mitigation
590 foundations and abilities are weak due to limited levels of economic, social, technological and
591 educational development (Ge Y-G, Cui P, & Chen X-Q 2020). In addition, these countries are focusing
592 more on building their economies, while they are ignoring the construction of disaster prevention and
593 mitigation systems (Gray C and Mueller V 2012; Jongman B, Ward PJ, & Aerts JCJH 2012; Tanoue M,
594 Hirabayashi Y, & Ikeuchi H 2016). In the cities and regions that are more susceptible to disasters,
595 regardless of whether the risks are to human lives or the economy, the prevention and mitigation of floods
596 should be emphasized. Subsequently, flood awareness should be increased to help deal with flood risks
597 in a sustainable way (Johnson C, Penning-Rowsell E, & Tapsell S 2007). Currently, more reliable
598 vulnerability studies need to be conducted for the entire Belt and Road region, and this study contributes
599 to this need.

600 Despite progress being made via this study, there are limitations to this study. Initially, a larger
601 resolution was considered for use, e.g., 1×1 km or 0.5×0.5 km (Ding M-T, Heiser M, Hubl J, & Fuchs S
602 2016), but later it was found that there were hundreds of millions of grids corresponding to these
603 resolutions, which was a huge test for the experimental equipment used. Regrettably, we only conducted

the spatial analysis of the vulnerability, not the temporal analysis. In the present study, due to the large area of the Belt and Road region and the availability of data, some common indicators were not included, such as the literacy rate, cultural level, existing medical conditions, and unemployment rates (Ding M-T, Heiser M, Hubl J, & Fuchs S 2016; Hoque MA, Tasfia S, Ahmed N, & Pradhan B 2019; Lee S, Okazumi T, Kwak Y, & Takeuchi K 2015). Additionally, the GDP per capita data used was calculated by GDP and population data and may decrease the accuracy of the results. In fact, there is still a lack of a consistent set of metrics to measure flood vulnerability, because different scholars have different understandings of vulnerability (Janssen MA, Schoon ML, Ke W, & Börner K 2006; Liverman D and O'Brien K 1991). However, the index system is a vital step in flood vulnerability assessment (Ding M-T, Heiser M, Hubl J, & Fuchs S 2016; Lyu H-M, Zhou W-H, Shen S-L, & Zhou A-N 2020). Thus, future studies should consider the influences of these factors, and this aspect should prove to be an interesting topic.

6. Conclusions

In this study, we adopted the index-based system based on the TFN-AHP and the SVM model to conduct the vulnerability assessment for the Belt and Road region. As a result, the spatial patterns of the exposure indicate that the high-exposure areas are primarily distributed in areas with higher population densities, more built-up land, and relatively developed economies. Additionally, the results of the disaster reduction capability assessment suggest that the disaster reduction capabilities of the countries along the Belt and Road are inextricably linked to their socio-economic development. The higher disaster reduction capability areas are mainly concentrated in the major cities in the Belt and Road region, including Beijing, Shanghai, Hong Kong, Taipei, Bangkok, Jakarta, New Delhi, Riyadh, Abu Dhabi, and Cairo. On the basis

of the exposure and disaster reduction capability results, the vulnerability assessment was calculated using Eq. (9). According to the results, most of the areas of the Belt and Road region (47,105,300 km^2) have extremely low and low vulnerability, approximately accounting for 93% of the total area. The highly-vulnerable areas (accounting for 3.54%) are primarily distributed in southern and eastern China, northern India, most of Bangladesh, the Indus Valley in Pakistan, the Nile River Basin in Egypt, the central region of Indonesia, and the major cities in the Belt and Road region. Obviously, these highly vulnerable regions and cities coincide with the areas that are characterized by frequent economic activities and dense populations, indicating that areas with high populations and economic densities may be more susceptible to flood disasters in the future. Although this study has limitations in terms of the temporal scale and spatial resolution, the results for the high-vulnerability regions will hopefully encourage local government officials to pay attention to "hot spots" where more accurate analyses need to be conducted.

Acknowledgments

This study is supported by Strategic Priority Research Program of the Chinese Academy of Sciences (Grant No. XDA20030302), Key R & D project of Sichuan Science and Technology Department (Grant No. 21QYCX0016), National Flash Flood Investigation and Evaluation Project (Grant No. SHZH-IWHR-57), National Key R&D Program of China (2020YFD1100701), and the Science and Technology Project of Xizang Autonomous Region (Grant No. XZ201901-GA-07), Project form Science and Technology Bureau of Altay Region in Yili Kazak Autonomous Prefecture. The authors are grateful to this support.

References

Adger WN. (2006). Vulnerability. Global Environmental Change, 16(3), 268-281.

https://dx.doi.org/10.1016/j.gloenvcha.2006.02.006
Adikari Y, Osti R, & Noro T. (2010). Flood-related disaster vulnerability: an impending crisis of megacities in Asia. Journal of Flood Risk Management, 3(3), 185-191. https://dx.doi.org/10.1111/j.1753-318X.2010.01068.x
An Y, Tan X-C, Gu B-H, & Zhu K-W. Flood risk assessment using the CV-TOPSIS method for the Belt and Road Initiative: an empirical study of Southeast Asia. Ecosystem Health and Sustainability, 6(1). https://dx.doi.org/10.1080/20964129.2020.1765703
Bodoque JM, Amerigo M, Díez-Herrero A, et al. (2016). Improvement of resilience of urban areas by integrating social perception in flash-flood risk management. Journal of Hydrology, 541, 665-676. https://dx.doi.org/10.1016/j.jhydrol.2016.02.005
Bouwer LM, Bubeck P, & Aerts JCJH. (2010). Changes in future flood risk due to climate and development in a Dutch polder area. Global Environmental Change, 20(3), 463-471. https://dx.doi.org/10.1016/j.gloenvcha.2010.04.002
Bui DT, Pradhan B, Lofman O, & Revhaug I. (2012). Landslide Susceptibility Assessment in Vietnam Using Support Vector Machines, Decision Tree, and Naive Bayes Models. Mathematical Problems in Engineering, 2012, 26. https://dx.doi.org/10.1155/2012/974638
Cascini L. (2008). Applicability of landslide susceptibility and hazard zoning at different scales. Engineering Geology, 102(3-4), 164-177. https://dx.doi.org/10.1016/j.enggeo.2008.03.016
Chen H-L, Ito Y, Sawamukai M, & Tokunaga T. (2015). Flood hazard assessment in the Kujukuri Plain of Chiba Prefecture, Japan, based on GIS and multicriteria decision analysis. Natural Hazards, 78(1), 105-120. https://dx.doi.org/10.1007/s11069-015-1699-5
Cheng Z-L, Zhou W-H, & Garg A. (2020). Genetic programming model for estimating soil suction in shallow soil layers in the vicinity of a tree. Engineering Geology, 268, 105506. https://doi.org/10.1016/j.enggeo.2020.105506
Cherkassky V. (1997). The Nature Of Statistical Learning Theory. IEEE Transactions on Neural Networks, 8(6), 1564-1564. https://dx.doi.org/10.1109/TNN.1997.641482
Cui P, Wu S-N, Lei Y, Zhang Z-T, & Zou Q. (2020). Disaster risk management pattern alongthe Belt and Roadregions. Science & Technology Review, 38(16), 35-44. https://dx.doi.org/10.3981/j.issn.1000-7857.2020.16.004
Cutter SL, & Finch C. (2008). Temporal and spatial changes in social vulnerability to natural hazards. Proceedings of the National Academy of ences, 105(7), 2301-2306. https://dx.doi.org/10.1073/pnas.0710375105
de Moel H, & Aerts JCJH. (2011). Effect of uncertainty in land use, damage models and inundation depth on flood damage estimates. Natural Hazards, 58(1), 407-425. https://dx.doi.org/10.1007/s11069-010-9675-6

687 Ding M-T, Heiser M, Hubl J, & Fuchs S. (2016). Regional vulnerability assessment for
688 debris flows in China—a CWS approach. Landslides, 13(3), 537-550.
689 https://dx.doi.org/10.1007/s10346-015-0578-1
690 Erena SH, & Worku H. (2019). Urban flood vulnerability assessments: the case of Dire
691 Dawa city, Ethiopia. Natural Hazards, 97(2), 495-516.
692 https://dx.doi.org/10.1007/s11069-019-03654-9
693 Eric N, & Thomas P. (2007). The Gendered Nature of Natural Disasters: The Impact of
694 Catastrophic Events on the Gender Gap in Life Expectancy, 1981–2002. Annals
695 of the American Association of Geographers, 97(3), 551-566.
696 https://dx.doi.org/10.1111/j.1467-8306.2007.00563.x
697 Fang Y, Yin J, & Wu B-H. (2016). Flooding risk assessment of coastal tourist attractions
698 affected by sea level rise and storm surge: a case study in Zhejiang Province,
699 China. Natural Hazards, 84(1), 611-624. https://dx.doi.org/10.1007/s11069-
700 016-2444-4
701 Fekete A. (2012). Spatial disaster vulnerability and risk assessments: challenges in their
702 quality and acceptance. Natural Hazards, 61(3), 1161-1178.
703 https://dx.doi.org/10.1007/s11069-011-9973-7
704 Franklin J. (2005). The elements of statistical learning: data mining, inference and
705 prediction. The Mathematical Intelligencer, 27(2), 83-85.
706 https://dx.doi.org/10.1007/BF02985802
707 Fraser EDG, Dougill AJ, Mabee WE, Reed M, & Mcalpine P. (2006). Bottom up and
708 top down: analysis of participatory processes for sustainability indicator
709 identification as a pathway to community empowerment and sustainable
710 environmental management. Journal of Environmental Management, 78(2),
711 114-127. https://dx.doi.org/10.1016/j.jenvman.2005.04.009
712 Gallopín G. (2006). Linkages between vulnerability, resilience, and adaptive capacity.
713 Global Environmental Change, 16(3), 293-303.
714 https://dx.doi.org/10.1016/j.gloenvcha.2006.02.004
715 Ge Y-G, Cui P, & Chen X-Q. (2020). Strategy of the international cooperation with
716 respect to disaster prevention and reduction in the Belt and Road areas. Science
717 & Technology Review, 38(16), 29-34. https://dx.doi.org/10.3981/j.issn.1000-
718 7857.2020.16.003
719 Gray C, & Mueller V. (2012). Drought and Population Mobility in Rural Ethiopia.
720 World Development, 40(1), 134-145.
721 https://doi.org/10.1016/j.worlddev.2011.05.023
722 He Y-Y, Zhou J-Z, Kou P-G, Lu N, & Zou Q. (2011). A fuzzy clustering iterative model
723 using chaotic differential evolution algorithm for evaluating flood disaster.
724 Expert Systems with Applications, 38(8), 10060-10065.
725 https://doi.org/10.1016/j.eswa.2011.02.003
726 Hoque MA, Tasfia S, Ahmed N, & Pradhan B. (2019). Assessing Spatial Flood
727 Vulnerability at Kalapara Upazila in Bangladesh Using an Analytic Hierarchy

728 Process. Sensors, 19(6), 1302. https://dx.doi.org/10.3390/s19061302
729 Hu P, Zhang Q, Shi P-J, Chen B, & Fang J-Y. (2018). Flood-induced mortality across
730 the globe: Spatiotemporal pattern and influencing factors. Science of The Total
731 Environment, 643, 171-182. https://doi.org/10.1016/j.scitotenv.2018.06.197
732 Huang J-Y, Liu Y, & Ma L. (2011). Assessment of regional vulnerability to natural
733 hazards in China using a DEA model. International Journal of Disaster Risk
734 ence, 2(2), 41-48. https://dx.doi.org/10.1007/s13753-011-0010-y
735 Janssen MA, Schoon ML, Ke W, & Börner K. (2006). Scholarly networks on resilience,
736 vulnerability and adaptation within the human dimensions of global
737 environmental change. Global Environmental Change, 16(3), 240-252.
738 https://doi.org/10.1016/j.gloenvcha.2006.04.001
739 Johnson C, Penning-Rowsell E, & Tapsell S. (2007). Aspiration and reality: flood policy,
740 economic damages and the appraisal process. Area, 39(2), 214-223.
741 https://dx.doi.org/10.1111/j.1475-4762.2007.00727.x
742 Jongman B, Ward PJ, & Aerts JCJH. (2012). Global exposure to river and coastal
743 flooding: Long term trends and changes. Global Environmental Change, 22(4),
744 823-835. https://doi.org/10.1016/j.gloenvcha.2012.07.004
745 Kim ES, & Choi HI. (2011). Assessment of Vulnerability to Extreme Flash Floods in
746 Design Storms. International Journal of Environmental Research & Public
747 Health, 8(7), 2907-2922. https://dx.doi.org/10.3390/ijerph8072907
748 Komolafe AA, Herath S, & Avtar R. (2019). Establishment of detailed loss functions
749 for the urban flood risk assessment in Chao Phraya River basin, Thailand.
750 Geomatics Natural Hazards & Risk, 10(1), 633-650.
751 https://dx.doi.org/10.1080/19475705.2018.1539038
752 Kummu M, Taka M, & Guillaume JHA. (2018). Data Descriptor: Gridded global
753 datasets for Gross Domestic Product and Human Development Index over
754 1990-2015. Scientific Data, 5, 15. https://dx.doi.org/10.1038/sdata.2018.4
755 Lee S, Okazumi T, Kwak Y, & Takeuchi K. (2015). Vulnerability proxy selection and
756 risk calculation formula for global flood risk assessment: a preliminary study.
757 Water Policy, 17(1), 8. https://dx.doi.org/10.2166/wp.2014.158
758 Li L-T, Xu Z-X, Pang B, & Liu L. (2012). Flood risk zoning in China. Journal of
759 Hydraulic Engineering, 43(1), 22-30.
760 https://dx.doi.org/10.13243/j.cnki.slxb.2012.01.001
761 Li Z-H, Nadim F, Huang H-W, Uzielli M, & Lacasse S. (2010). Quantitative
762 vulnerability estimation for scenario-based landslide hazards. Landslides, 7(2),
763 125-134. https://dx.doi.org/10.1007/s10346-009-0190-3
764 Liu J-F, Wang X-Q, Zhang B, Li J, Zhang J-Q, & Liu X-Q. (2017). Storm flood risk
765 zoning in the typical regions of Asia using GIS technology. Natural Hazards,
766 87(3), 1691-1707. https://dx.doi.org/10.1007/s11069-017-2843-1
767 Liu J, & Wang S-Y. (2013). Analysis of human vulnerability to the extreme rainfall
768 event on 21–22 July 2012 in Beijing, China. Natural Hazards Earth System

769 Science, 13(11), 2911-2926. https://dx.doi.org/10.5194/nhess-13-2911-2013
770 Liu X-L, Cheng M, & Tian C-S. (2017). Comparative Analysis of Two Methods for
771 Assessing Hazard of Landslide and Debris-flow on a Regional Scale. Journal of
772 Disaster Prevention Mitigation Engineering.
773 https://dx.doi.org/10.13409/j.cnki.jdpme.2017.01.010
774 Liu X-L, & Lei J-Z. (2003). A method for assessing regional debris flow risk: an
775 application in Zhaotong of Yunnan province (SW China). Geomorphology.
776 https://dx.doi.org/10.1016/S0169-555X(02)00242-8
777 Liu Y-S, Yang Z-S, Huang Y-H, & Liu C-J. (2018). Spatiotemporal evolution and
778 driving factors of China's flash flood disasters since 1949. Science China-Earth
779 Sciences, 61(12), 1804-1817. https://dx.doi.org/10.1007/s11430-017-9238-7
780 Liverman D, & O'Brien K. (1991). Global warming and climate change in Mexico.
781 Global Environmental Change, 1(5), 351-364. https://dx.doi.org/10.1016/0959-
782 3780(91)90002-B
783 Lugeri N, Kundzewicz ZW, Genovese E, Hochrainer S, & Radziejewski M. (2010).
784 River flood risk and adaptation in Europe—assessment of the present status.
785 Mitigation and Adaptation Strategies for Global Change, 15(7), 621-639.
786 https://dx.doi.org/10.1007/s11027-009-9211-8
787 Lyu H-M, Shen S-L, Yang J, & Yin Z-Y. (2019). Inundation analysis of metro systems
788 with the storm water management model incorporated into a geographical
789 information system: a case study in Shanghai. HYDROLOGY AND EARTH
790 SYSTEM SCIENCES, 23(10), 4293-4307. https://dx.doi.org/10.5194/hess-23-
791 4293-2019
792 Lyu H-M, Shen S-L, Zhou A-N, & Yang J. (2020). Risk assessment of mega-city
793 infrastructures related to land subsidence using improved trapezoidal FAHP.
794 Science of The Total Environment, 717, 135310.
795 https://doi.org/10.1016/j.scitotenv.2019.135310
796 Lyu H-M, Shen S-L, Zhou A-N, & Zhou W-H. (2019). Flood risk assessment of metro
797 systems in a subsiding environment using the interval FAHP-FCA approach.
798 Sustainable Cities and Society, 50, 101682.
799 https://doi.org/10.1016/j.scs.2019.101682
800 Lyu H-M, Zhou W-H, Shen S-L, & Zhou A-N. (2020). Inundation risk assessment of
801 metro system using AHP and TFN-AHP in Shenzhen. Sustainable Cities, 56,
802 102103. https://dx.doi.org/10.1016/j.scs.2020.102103
803 Mahmoud SH, & Gan TY. (2018). Multi-criteria approach to develop flood
804 susceptibility maps in arid regions of Middle East. Journal of Cleaner
805 Production, 196, 216-229. https://dx.doi.org/10.1016/j.jclepro.2018.06.047
806 Malone EL, & Engle NL. (2011). Evaluating regional vulnerability to climate change:
807 purposes and methods. Wiley Interdisciplinary Reviews Climate Change, 2(3),
808 462-474. https://dx.doi.org/10.1002/wcc.116
809 Metzger MJ, Rounsevell MDA, Acosta-Michlik L, Leemans R, & Schröter D. (2006).

The Vulnerability of Ecosystem Services to Land Use Change. Agriculture Ecosystems & Environment, 114(1), 69-85. https://dx.doi.org/10.1016/j.agee.2005.11.025

Njock PGA, Shen S-L, Zhou A-N, & Lyu H-M. (2020). Evaluation of soil liquefaction using AI technology incorporating a coupled ENN / t-SNE model. Soil Dynamics and Earthquake Engineering, 130, 105988. https://doi.org/10.1016/j.soildyn.2019.105988

Ntajal J, Lamptey BL, Mahamadou IB, & Nyarko BK. (2017). Flood disaster risk mapping in the Lower Mono River Basin in Togo, West Africa. International Journal of Disaster Risk Reduction, 23, 93-103. https://doi.org/10.1016/j.ijdrr.2017.03.015

Okazawa Y, Yeh PJF, Kanae S, & Oki T. (2011). Development of a global flood risk index based on natural and socio-economic factors. International Association of entific Hydrology Bulletin, 56(5), 789-804. https://dx.doi.org/10.1080/02626667.2011.583249

Rana IA, & Routray JK. (2018). Integrated methodology for flood risk assessment and application in urban communities of Pakistan. Natural Hazards, 91(1), 239 - 266. https://dx.doi.org/10.1007/s11069-017-3124-8

Rani NNVS, Satyanarayana ANV, & Bhaskaran PK. (2015). Coastal vulnerability assessment studies over India: a review. Natural Hazards, 77(1), 405-428. https://dx.doi.org/10.1007/s11069-015-1597-x

Rawat PK, Pant CC, Tiwari PC, & Sharma PDPK. (2012). Spatial variability assessment of river-line floods and flash floods in Himalaya. Disaster Prevention Management, 21(2), 135-159. http://dx.doi.org/10.1108/09653561211219955

Rimba AB, Setiawati MD, Sambah AB, & Miura F. (2017). Physical Flood Vulnerability Mapping Applying Geospatial Techniques in Okazaki City, Aichi Prefecture, Japan. Urban Science, 1(7), 1-22. https://dx.doi.org/10.3390/urbansci1010007

Sam AS, Kumar R, Kachele H, & Muller K. (2017). Vulnerabilities to flood hazards among rural households in India. Natural Hazards, 88(2), 1133 -1153. https://dx.doi.org/10.1007/s11069-017-2911-6

Sampson CC, Fewtrell TJ, Duncan A, Shaad K, Horritt MS, & Bates PD. (2012). Use of terrestrial laser scanning data to drive decimetric resolution urban inundation models. Advances in Water Resources, 41, 1-17. https://dx.doi.org/10.1016/j.advwatres.2012.02.010

Sharma SVS, Roy PS, Chakravarthi V, & Rao GS. (2017). Flood risk assessment using multi-criteria analysis: a case study from Kopili River Basin, Assam, India. Geomatics Natural Hazards Risk(1), 1-15. https://dx.doi.org/10.1007/s11069-015-1597-x

Shi Y. (2013). Population vulnerability assessment based on scenario simulation of

851 rainstorm-induced waterlogging: a case study of Xuhui District, Shanghai City.
852 Natural Hazards, 66(2), 1189-1203. https://dx.doi.org/10.1007/s11069-012-
853 0544-3
854 Shi Y, Xu S-Y, & Shi C. (2011). Progress in research on vulnerability of natural disasters.
855 Journal of Natural Disasters, 20(02), 131-137.
856 https://dx.doi.org/10.13577/j.jnd.2011.0221
857 Spitalar M, Gourley JJ, Lutoff C, Kirstetter PE, Brilly M, & Carr N. (2014). Analysis
858 of flash flood parameters and human impacts in the US from 2006 to 2012.
859 Journal of Hydrology, 519, 863-870.
860 https://doi.org/10.1016/j.jhydrol.2014.07.004
861 Susan L, & Cutter. (2003). Social Vulnerability to Environmental Hazards. Social
862 Science Quarterly. https://dx.doi.org/10.1111/1540-6237.8402002
863 Tanoue M, Hirabayashi Y, & Ikeuchi H. (2016). Global-scale river flood vulnerability
864 in the last 50 years. Scientific Reports, 6, 9.
865 https://dx.doi.org/10.1038/srep36021
866 Tehrany MS, Pradhan B, & Jebur MN. (2013). Spatial prediction of flood susceptible
867 areas using rule based decision tree (DT) and a novel ensemble bivariate and
868 multivariate statistical models in GIS. Journal of Hydrology, 504, 69-79.
869 https://dx.doi.org/10.1016/j.jhydrol.2013.09.034
870 Tehrany MS, Pradhan B, & Jebur MN. (2014). Flood susceptibility mapping using a
871 novel ensemble weights-of-evidence and support vector machine models in GIS.
872 Journal of Hydrology, 512(6), 332-343.
873 https://dx.doi.org/10.1016/j.jhydrol.2014.03.008
874 Tehrany MS, Pradhan B, Mansor S, & Ahmad N. (2015). Flood susceptibility
875 assessment using GIS-based support vector machine model with different kernel
876 types. Catena, 125, 91-101. https://dx.doi.org/10.1016/j.catena.2014.10.017
877 Wan SA, & Lei TC. (2009). A knowledge-based decision support system to analyze the
878 debris-flow problems at Chen-Yu-Lan River, Taiwan. Knowledge-Based
879 Systems, 22(8), 580-588. https://dx.doi.org/10.1016/j.knosys.2009.07.008
880 Weis SWM, Agostini VN, Roth LM, et al. (2016). Assessing vulnerability: an integrated
881 approach for mapping adaptive capacity, sensitivity, and exposure. Climatic
882 Change, 136(3), 615-629. https://dx.doi.org/10.1007/s10584-016-1642-0
883 Werren G, Reynard E, Lane SN, & Balin D. (2016). Flood hazard assessment and
884 mapping in semi-arid piedmont areas: a case study in Beni Mellal, Morocco.
885 Natural Hazards, 81(1), 481-511. https://dx.doi.org/10.1007/s11069-015-2092-
886 0
887 Wu J, Yang R, & Song J. (2018). Effectiveness of low-impact development for urban
888 inundation risk mitigation under different scenarios: a case study in Shenzhen,
889 China. NATURAL HAZARDS AND EARTH SYSTEM SCIENCES, 18(9),
890 2525-2536. https://dx.doi.org/10.5194/nhess-18-2525-2018
891 Xia F-Q, Kang X-W, Wu S-H, et al. (2008). Research on dike breach risk of the hanging

reach under different flood conditions in the Lower Yellow River. Geographical Research, 27(1), 229-239. https://dx.doi.org/10.1016/S1005-8885(08)60096-5

Xian S-D. (2010). A new fuzzy comprehensive evaluation model based on the support vector machine. Fuzzy Information Engineering, 2(1), 75-86. https://dx.doi.org/10.1007/s12543-010-0038-5

Xiong J-N, Li J, Cheng W-M, Wang N, & Guo L. (2019). A GIS-Based Support Vector Machine Model for Flash Flood Vulnerability Assessment and Mapping in China. International Journal of Geo-Information, 8(7), 297. https://dx.doi.org/10.3390/ijgi8070297

Xiong J-N, Sun M, Zhang H, et al. (2019). Application of the Levenburg-Marquardt back propagation neural network approach for landslide risk assessments. NATURAL HAZARDS AND EARTH SYSTEM SCIENCES, 19(3), 629-653. https://dx.doi.org/10.5194/nhess-19-629-2019

Xu C, Dai F-C, Xu X-W, & Lee YH. (2012). GIS-based support vector machine modeling of earthquake-triggered landslide susceptibility in the Jianjiang River watershed, China. Geomorphology, 145-146, 70-80. https://dx.doi.org/10.1016/j.geomorph.2011.12.040

Yang X-L, Ding J-H, & Hou H. (2013). Application of a triangular fuzzy AHP approach for flood risk evaluation and response measures analysis. Natural Hazards, 68(2), 657-674. https://dx.doi.org/10.1007/s11069-013-0642-x

Yao X, Tham LG, & Dai F-C. (2008). Landslide susceptibility mapping based on Support Vector Machine: A case study on natural slopes of Hong Kong, China. Geomorphology, 101(4), 572-582. https://dx.doi.org/10.1016/j.geomorph.2008.02.011

Zhang J-D. (2018). The Current Situation of the One Belt and One Road Initiative and Its Development Trend. In Rong WZhu C-P (Eds.), *Annual Report on the Development of the Indian Ocean Region (2017): The Belt and Road Initiative and South Asia* (pp. 103-137). Singapore: Springer Singapore.

Zhang Y-L, & You W-J. (2014). Social vulnerability to floods: a case study of Huaihe River Basin. Natural Hazards, 71(3), 2113-2125. https://dx.doi.org/10.1007/s11069-013-0996-0

Zhang Z-G. (2014). Research on rainstorm waterlogging risk assessment of urban comminities——a case of Jinsha community, Shanghai. Shanghai Normal University.

Zhou J, Jiang T, Wang Y-J, Su B-D, & Zhai J-Q. (2020). Spatiotemporal variations of aridity index over the Belt and Road region under the 1.5°C and 2.0°C warming scenarios. Journal of Geographical ences, 30(1), 37-52. https://dx.doi.org/10.1007/s11442-020-1713-z

Zhou S-E, Zhang M-J, & Wang S-J. (2018). Assessment of vulnerability in natural-social system in Hexi, Gansu. Resources Science, 40(2), 452-462. https://dx.doi.org/10.18402/resci.2018.02.20

933 Zhou Y, Li N, Wu W-X, & Wu J-D. (2014). Assessment of provincial social
934 vulnerability to natural disasters in China. Natural Hazards, 71(3), 2165-2186.
935 https://dx.doi.org/10.1007/s11069-013-1003-5
936 Zong N. (2013). Flood hazard vulnerability and risk assessment of urban community——A case study of Shanghai. East China Normal University.

938

939 **LIST OF TABLES AND FIGURES**

946

953

954 **Table 2** Sources and resolutions of the datasets

Factors	Source	Resolution	Type, Timeframe
Population	World Pop	1×1 km	raster data, 2015
Land use	National Aeronautics and Space Administration (NASA)	0.5×0.5 km	vector data, 2015
GDP	Dryad	5 arc-min	raster data, 2015
Infrastructure	OpenStreetMap	1:50,000	vector data, 2015
DEM	SRTM Data	1×1 km	raster data, 2010
Impervious surface	Global Human Settlement Layer (GHSL)	30×30 m	raster data, 2014

955

956 **Table 2** Linguistic variables and the corresponding triangular fuzzy numbers

Linguistic Terms	Intensity Importance	Triangular Fuzzy Numbers	Reciprocal Triangular Fuzzy Numbers
Equal importance	1`	(1,1,1)	(1,1,1)
Almost equal importance	1	(1,1,3)	(1/3,1,1)
Intermediate value	2	(1,2,4)	(1/4,1/2,1)
Moderate importance	3	(1,3,5)	(1/5,1/3,1)
Intermediate value	4	(2,4,6)	(1/6,1/4,1/2)
Strong importance	5	(3,5,7)	(1/7,1/5,1/3)
Intermediate value	6	(4,6,8)	(1/8,1/6,1/4)
Very strong importance	7	(5,7,9)	(1/9,1/7,1/5)
Intermediate value	8	(6,8,10)	(1/10,1/8,1/6)
Extreme importance	9	(7,9,11)	(1/11,1/9,1/7)

957 **Table 3** Judgment matrix and normalized weights of the exposure indexes

Exposure	FAD	BUD	ECD	POD	Normalized Weights
FAD	(1,1,1)	(0.5,1,1)	(0.2,0.333,1)	(0.143,0.2,0.333)	0.032
BUD	(1,1,2)	(1,1,1)	(0.333,0.5,1)	(0.2,0.25,0.5)	0.110
ECD	(1,3,5)	(1,2,3)	(1,1,1)	(0.25,0.5,1)	0.346
POD	(3,5,7)	(2,4,5)	(1,2,4)	(1,1,1)	0.512

958 **Note**: FAD is the farmland density; BUD is the building density; ECD is the economic density; and POD

959 is the population density.

960

961 **Table 4** Exposure of floods for the grid cells throughout the Belt and Road region

Type	Exposure		
	Count	Area/10000 km^2	Ratio (%)
Extremely low	558632	4378.15	86.45
Low	44006	344.62	6.81
Moderate	25977	203.57	4.02
High	13053	102.11	2.02
Extremely high	4523	35.59	0.70

962

963 **Table 5** Disaster reduction capability of floods for the grid cells throughout the Belt and Road region

Type	Disaster Reduction Capability		
	Count	Area/10000 km^2	Ratio (%)
Extremely low	520377	4078.53	80.53
Low	100418	786.92	15.54
Moderate	21065	164.94	3.26
High	3683	28.72	0.57
Extremely high	648	4.93	0.10

964

965 **Table 6** Vulnerability of floods for the grid cells throughout the Belt and Road region

Type	Vulnerability		
	Count	Area/10000 km^2	Ratio (%)
Extremely low	559149	4381.75	86.53
Low	41938	328.78	6.49
Moderate	22229	174.42	3.44
High	15767	123.61	2.44
Extremely high	7108	55.48	1.10

966

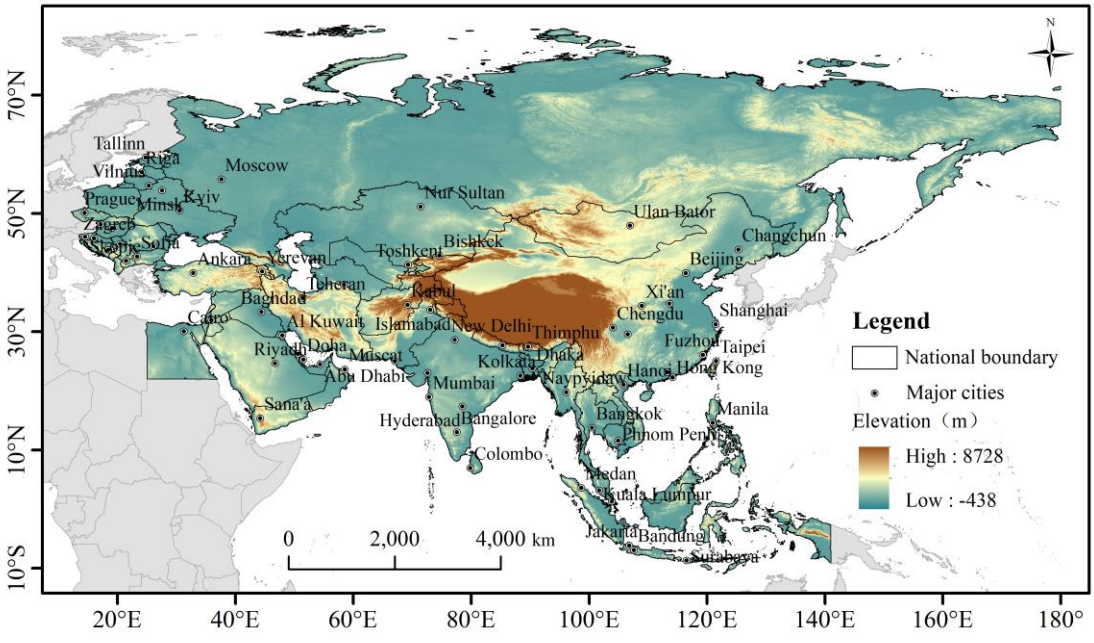

967

968 **Fig. 3** Location of the Belt and Road region

969

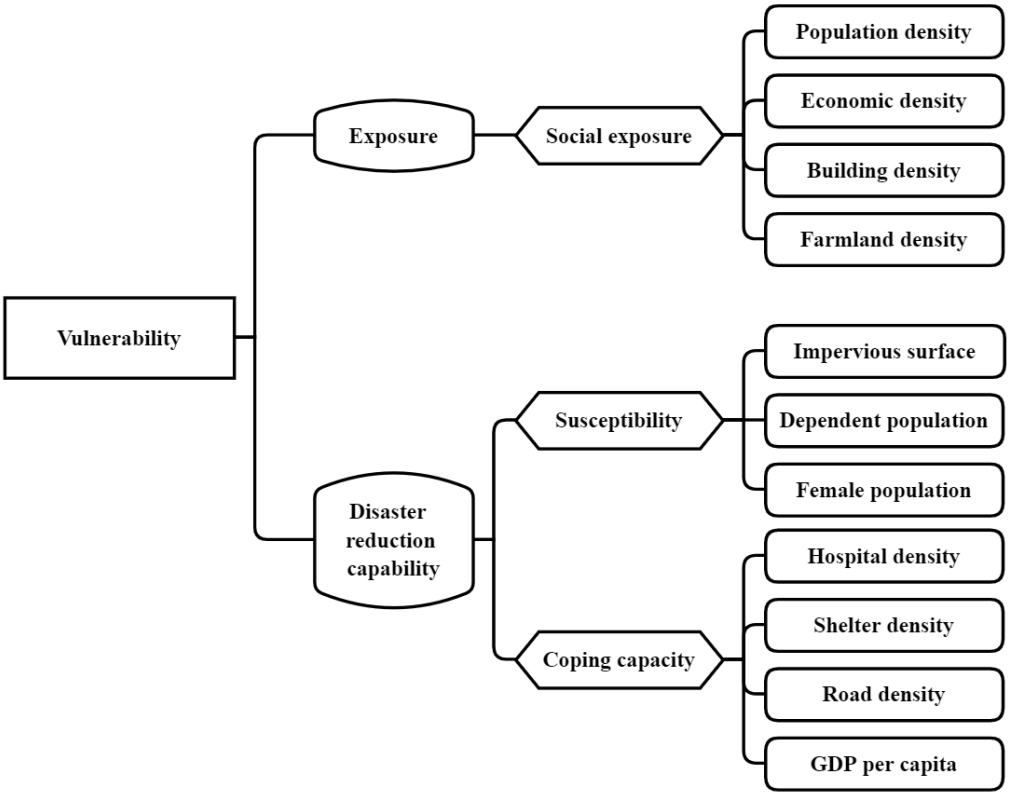

970

971 **Fig. 1** Flood vulnerability assessment index system for the Belt and Road region

972

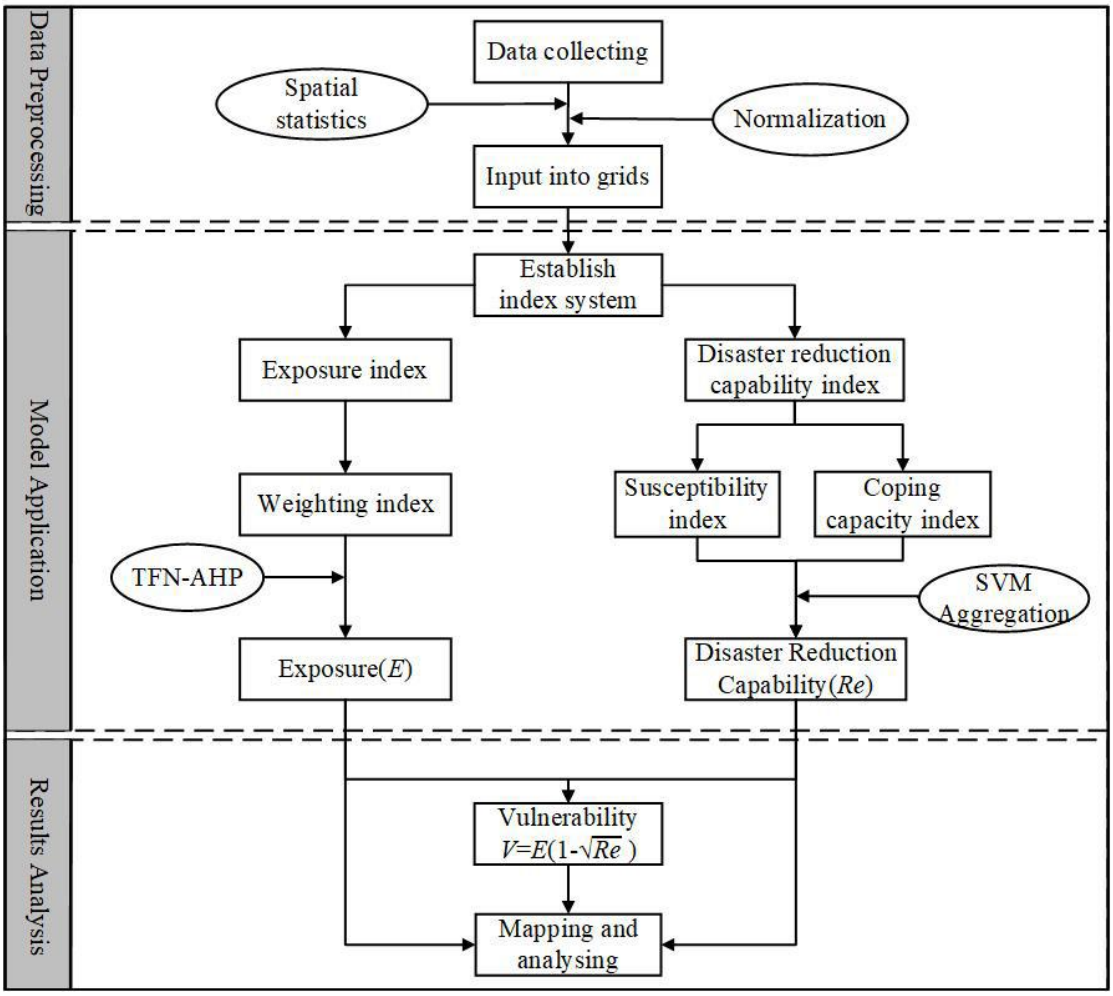

973

974 **Fig. 2** Flowchart of the flood vulnerability assessment throughout the Belt and Road region

975

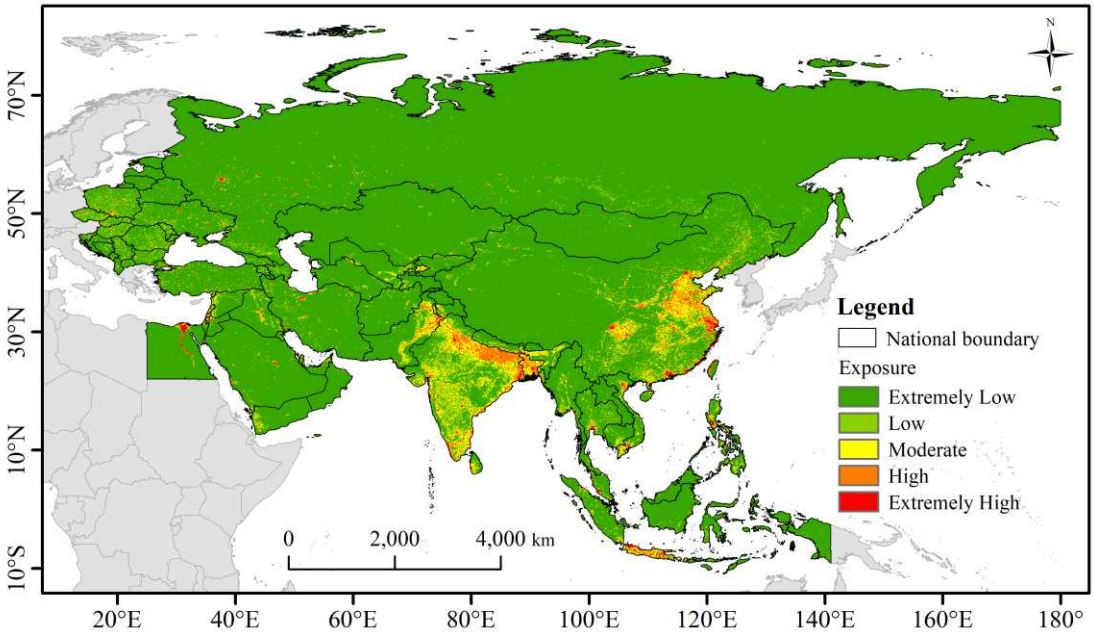

976

977 **Fig. 3** Spatial distribution of the exposure throughout the Belt and Road region

978

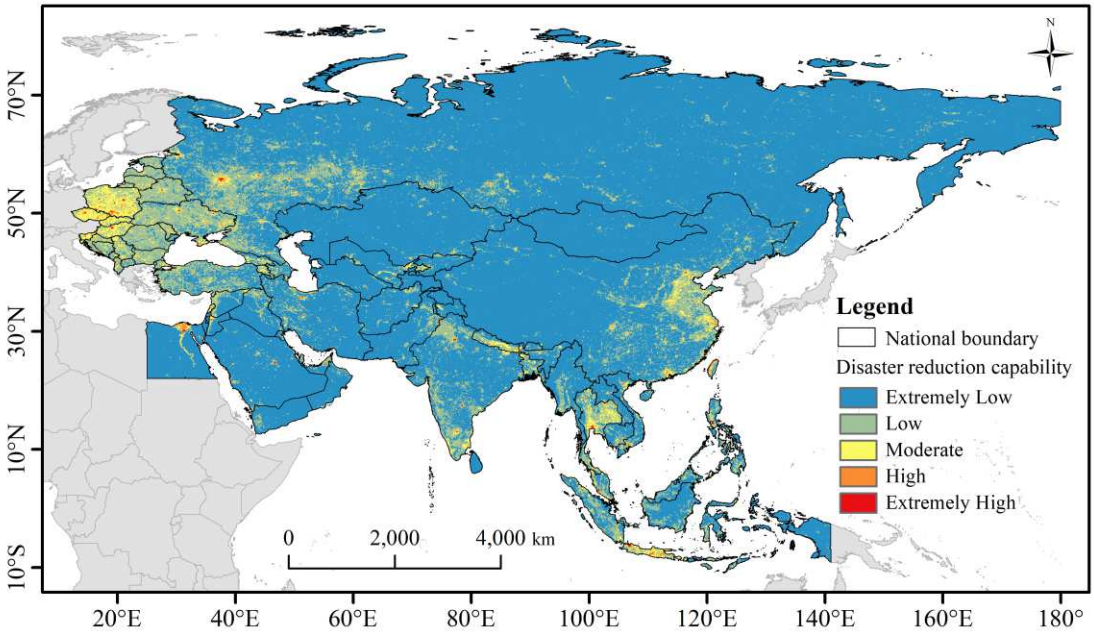

979

980 **Fig. 4** Spatial distribution of the disaster reduction capability throughout the Belt and Road region

981

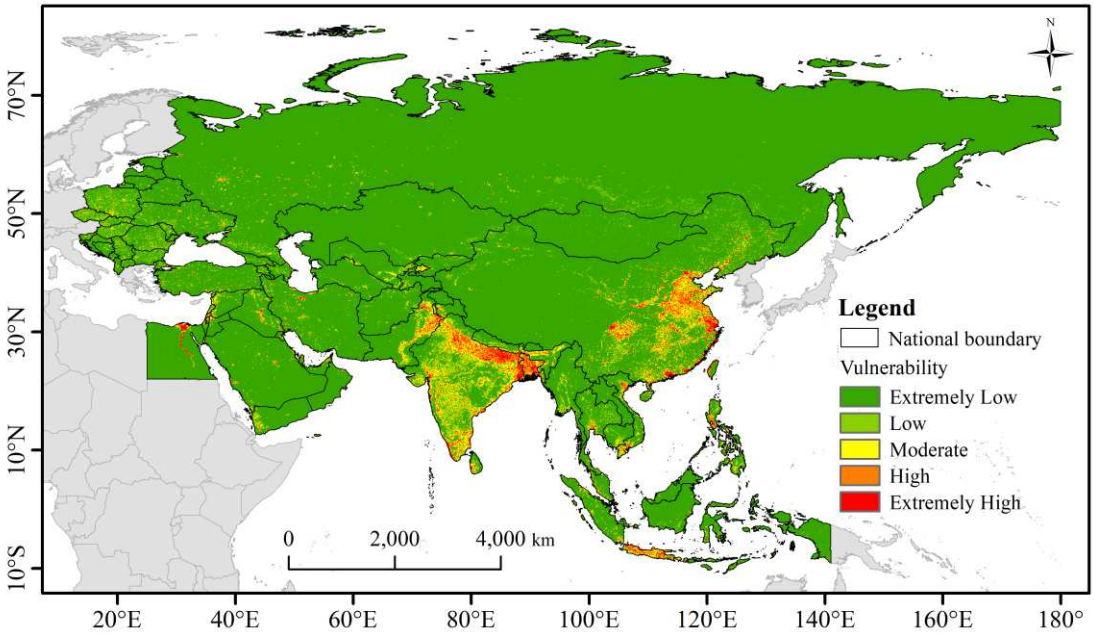

982

983 **Fig. 5** Spatial distribution of the vulnerability throughout the Belt and Road region

984

985

Figures

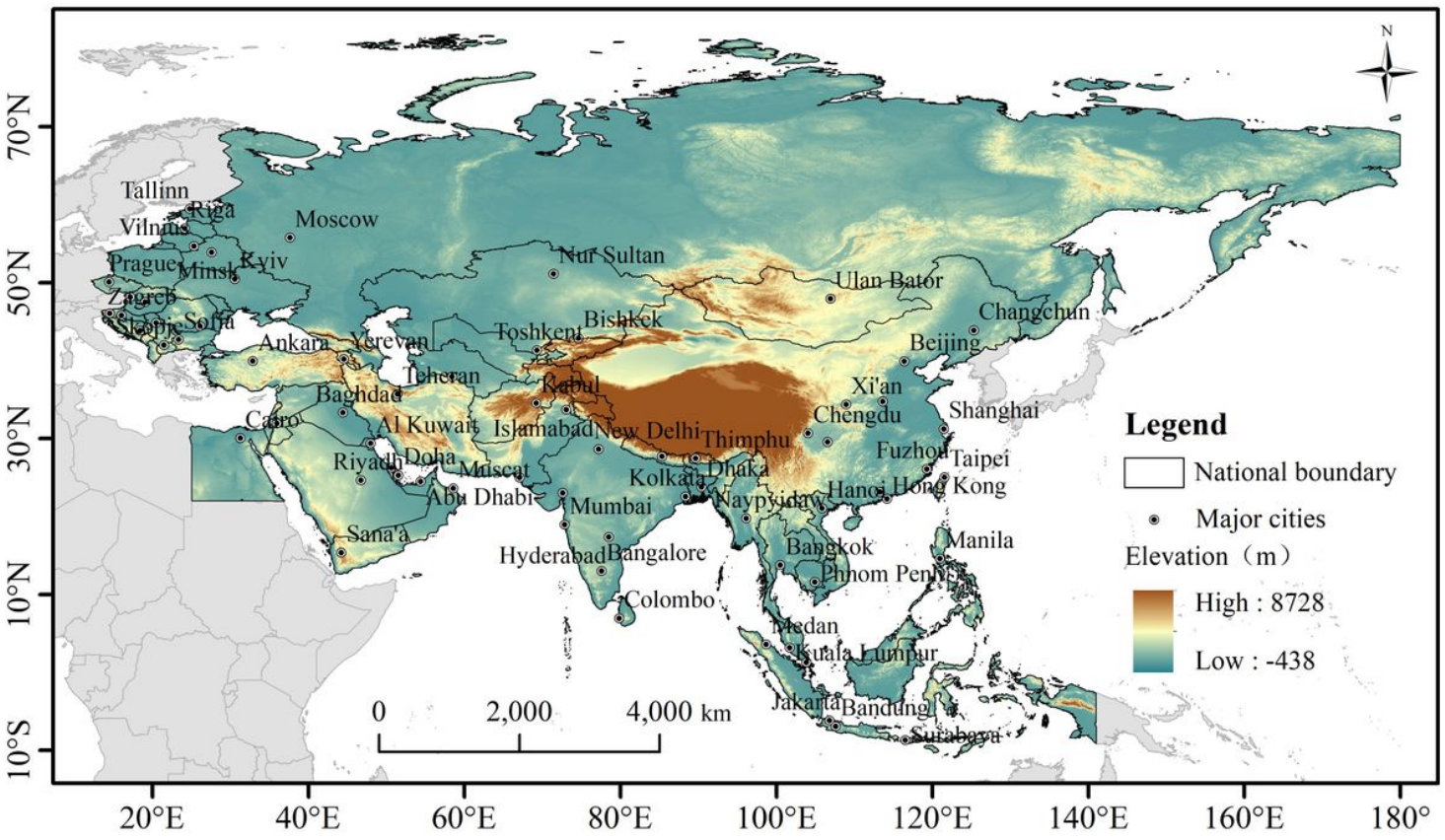

Figure 1

Location of the Belt and Road region. Note: The designations employed and the presentation of the material on this map do not imply the expression of any opinion whatsoever on the part of Research Square concerning the legal status of any country, territory, city or area or of its authorities, or concerning the delimitation of its frontiers or boundaries. This map has been provided by the authors.

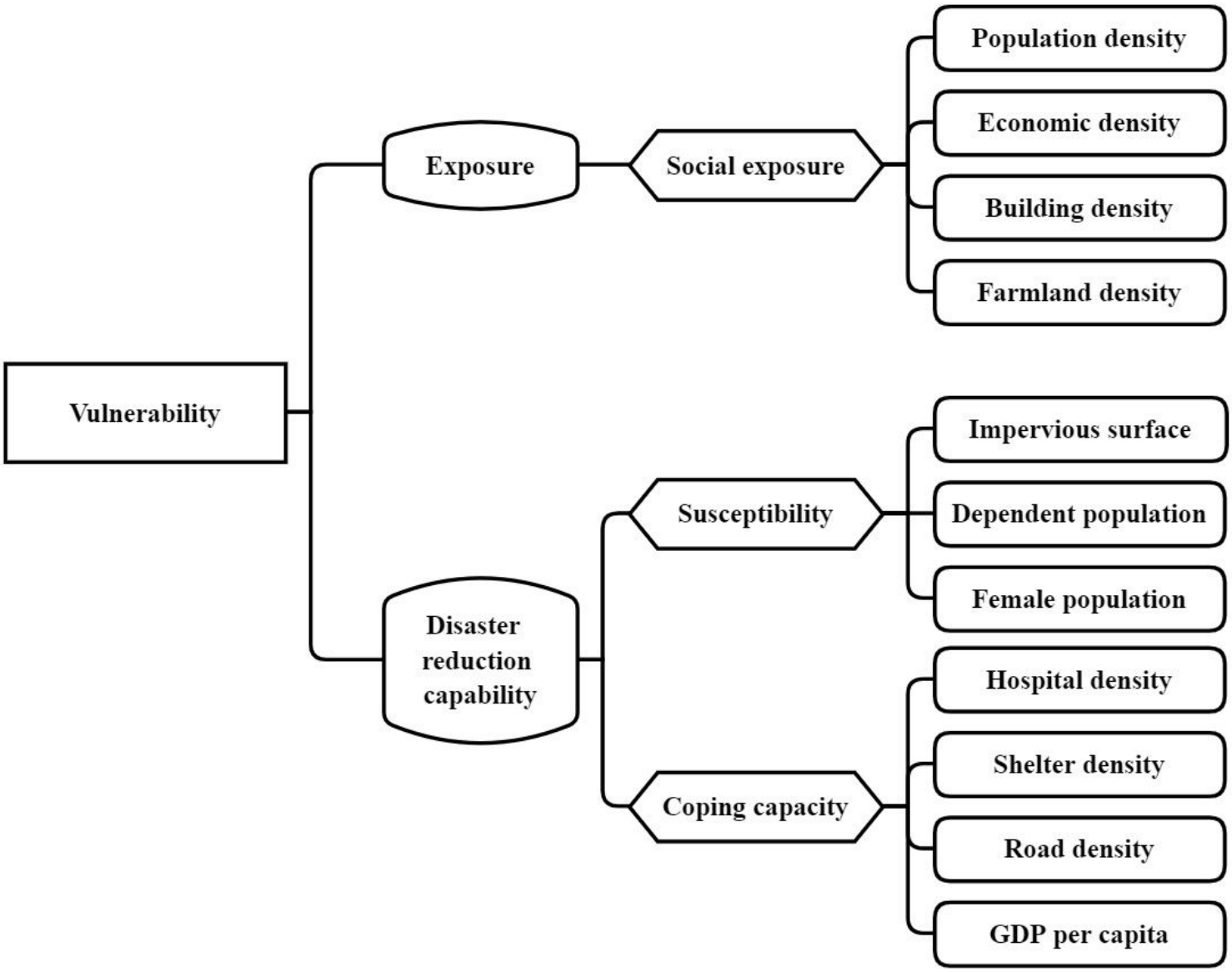

Figure 2

Flood vulnerability assessment index system for the Belt and Road region

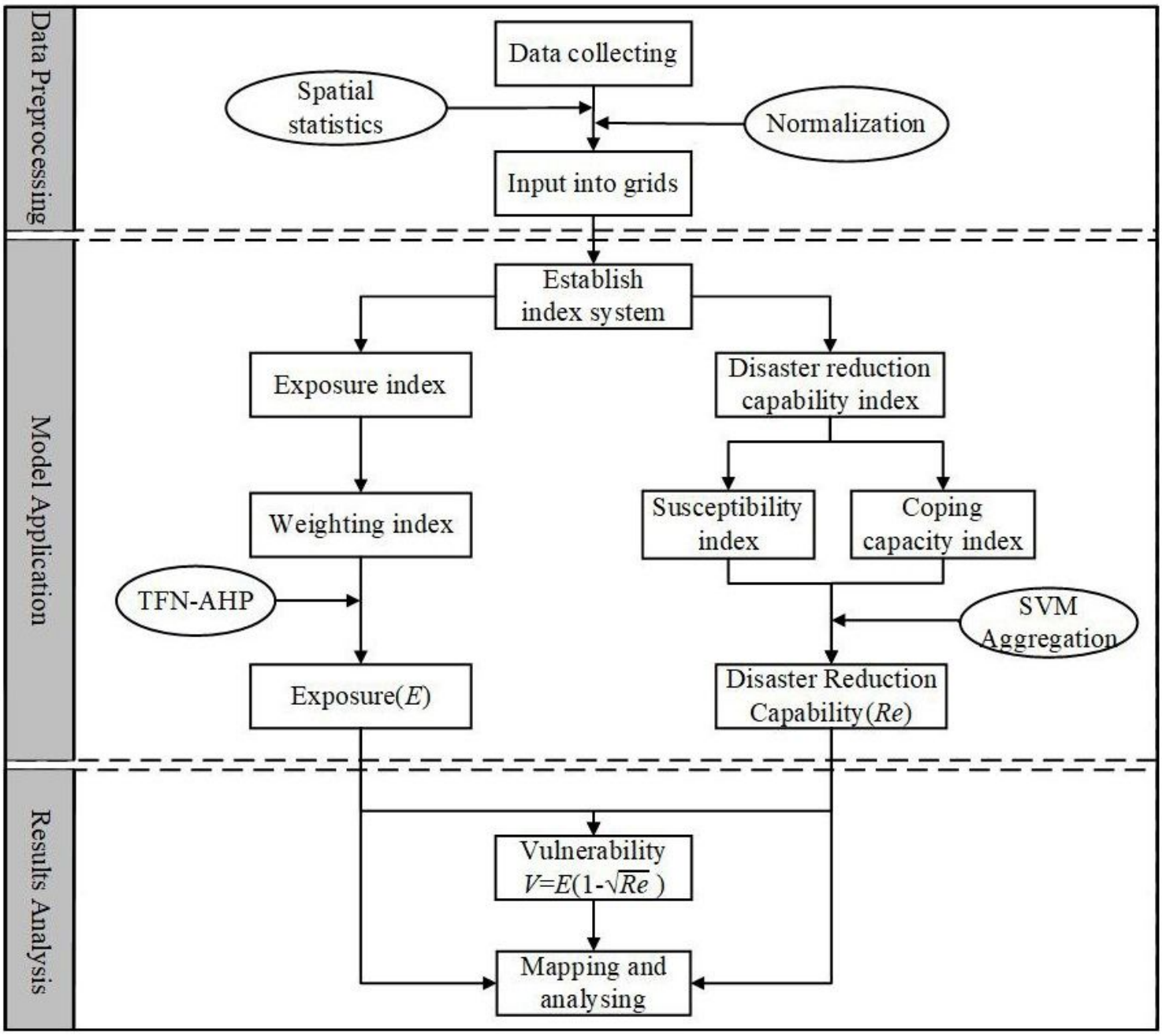

Figure 3

Flowchart of the flood vulnerability assessment throughout the Belt and Road region

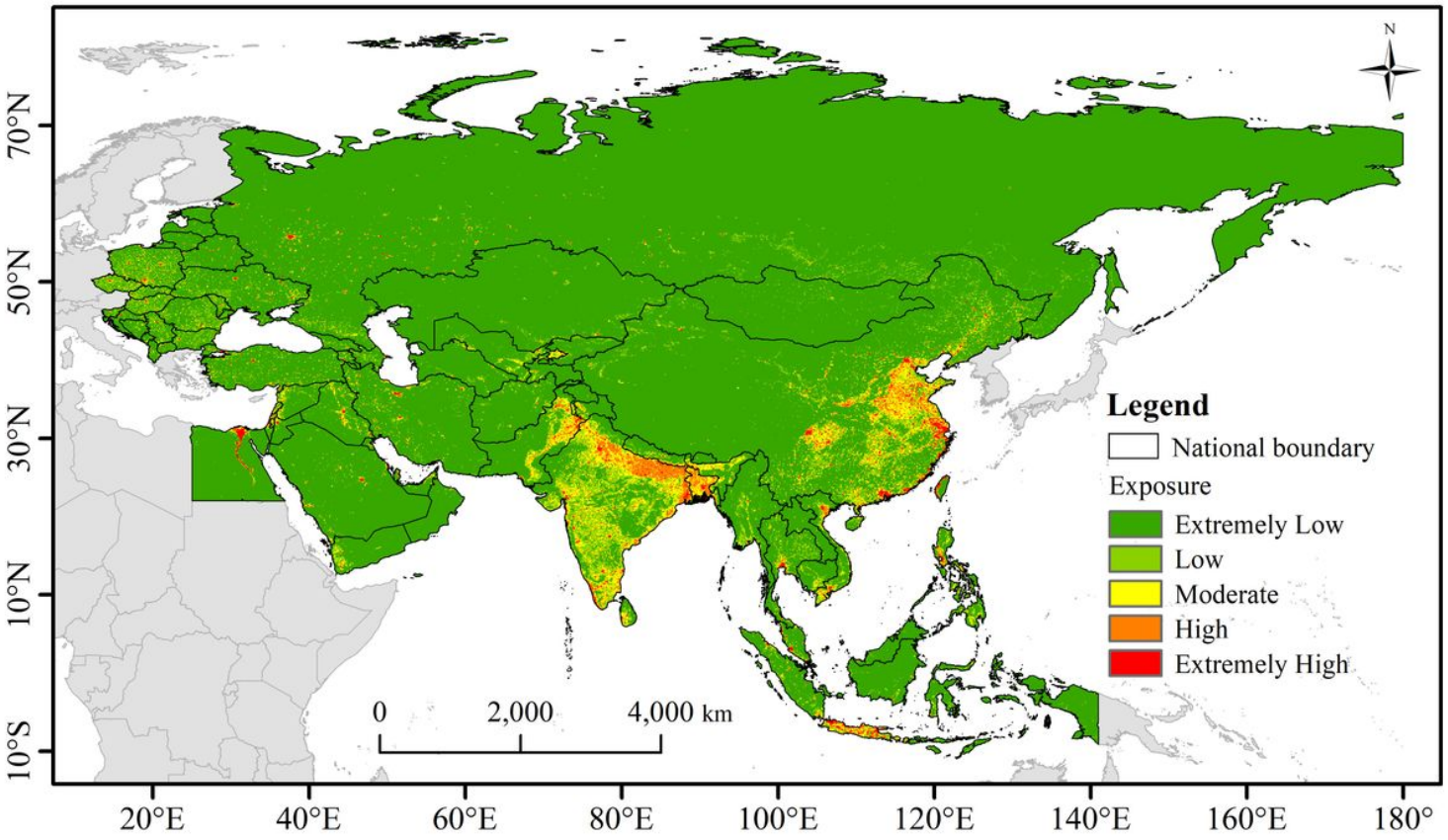

Figure 4

Spatial distribution of the exposure throughout the Belt and Road region. Note: The designations employed and the presentation of the material on this map do not imply the expression of any opinion whatsoever on the part of Research Square concerning the legal status of any country, territory, city or area or of its authorities, or concerning the delimitation of its frontiers or boundaries. This map has been provided by the authors.

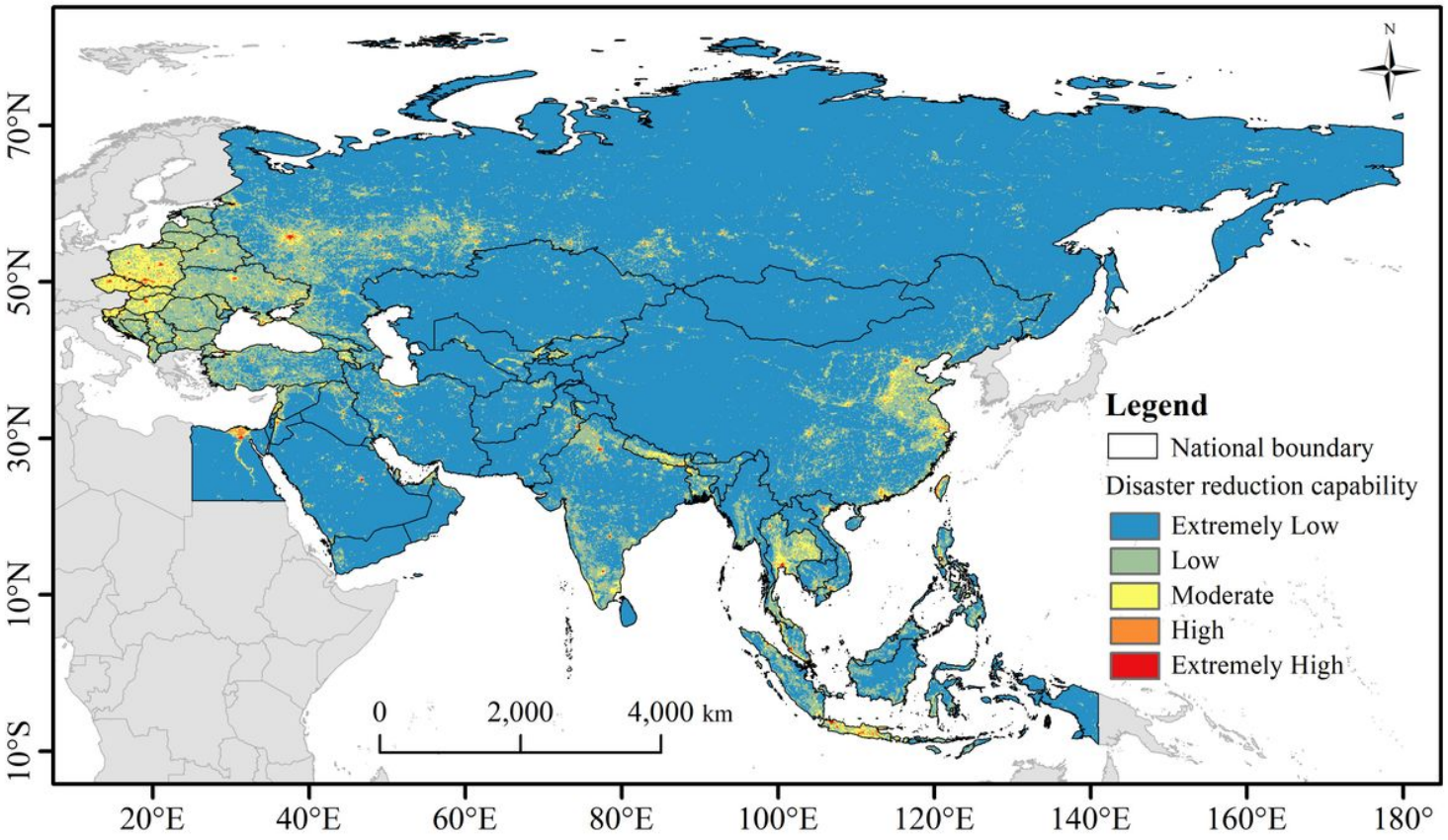

Figure 5

Spatial distribution of the disaster reduction capability throughout the Belt and Road region. Note: The designations employed and the presentation of the material on this map do not imply the expression of any opinion whatsoever on the part of Research Square concerning the legal status of any country, territory, city or area or of its authorities, or concerning the delimitation of its frontiers or boundaries. This map has been provided by the authors.

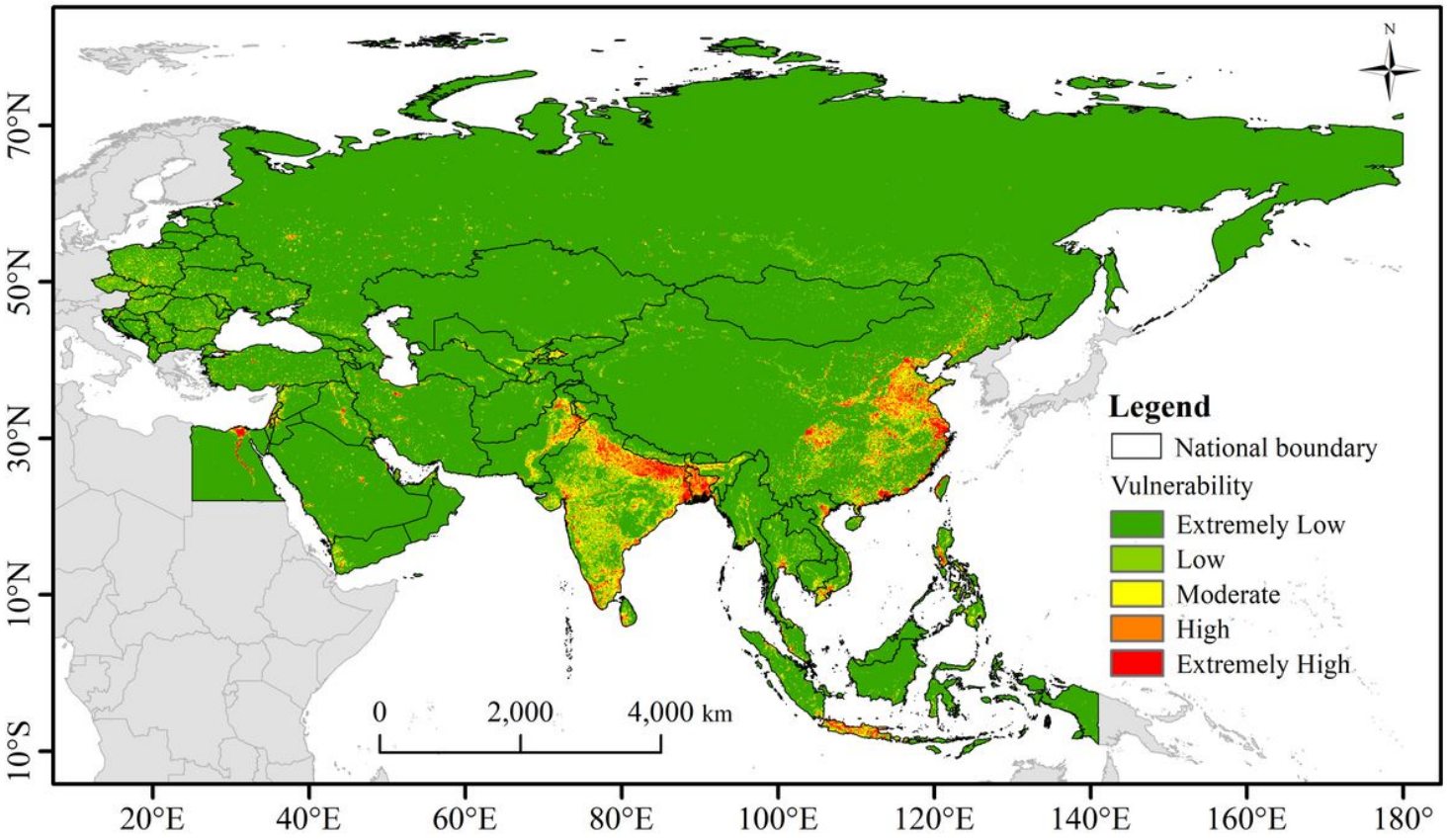

Figure 6

Spatial distribution of the vulnerability throughout the Belt and Road region. Note: The designations employed and the presentation of the material on this map do not imply the expression of any opinion whatsoever on the part of Research Square concerning the legal status of any country, territory, city or area or of its authorities, or concerning the delimitation of its frontiers or boundaries. This map has been provided by the authors.